

Introduction to Microelectronic Fabrication

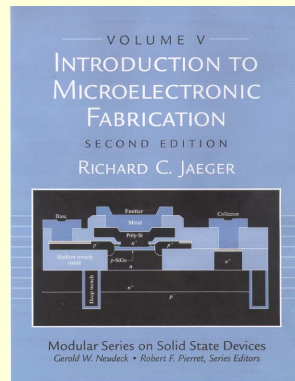
by

Richard C. Jaeger

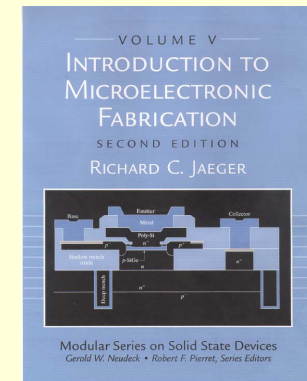
Distinguished University Professor
ECE Department

Auburn University

Chapter 4 Diffusion

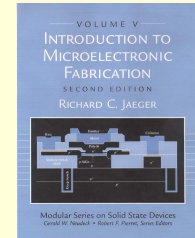


© 2002 Pearson Education, Inc., Upper Saddle River, NJ. All rights reserved.
This material is protected under all copyright laws as they currently exist. No
portion of this material may be reproduced, in any form or by any means,
without permission in writing from the publisher.



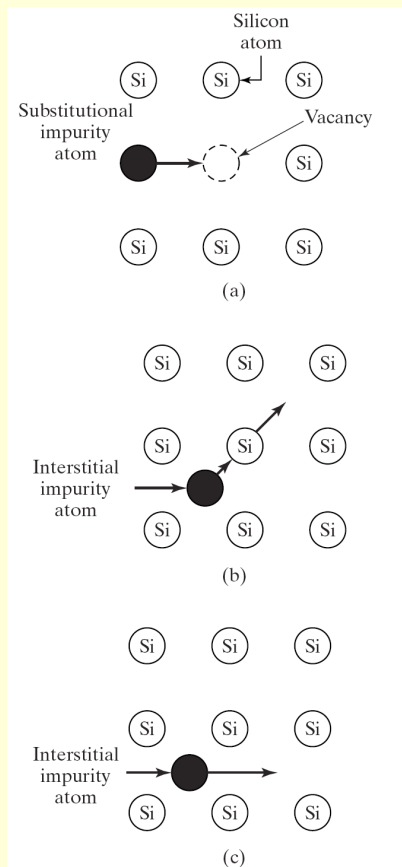
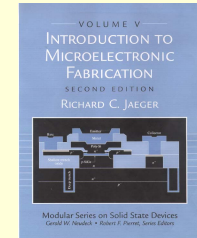
For the exclusive use of adopters of the book
Introduction to Microelectronic Fabrication,
Second Edition by Richard C. Jaeger. ISBN0-201-
44494-1.

Copyright Notice



- © 2002 Pearson Education, Inc., Upper Saddle River, NJ. All rights reserved. This material is protected under all copyright laws as they currently exist. No portion of this material may be reproduced, in any form or by any means, without permission in writing from the publisher.
- For the exclusive use of adopters of the book Introduction to Microelectronic Fabrication, Second Edition by Richard C. Jaeger. ISBN0-201-44494-1.

Impurity Diffusion



• Diffusion Mechanisms

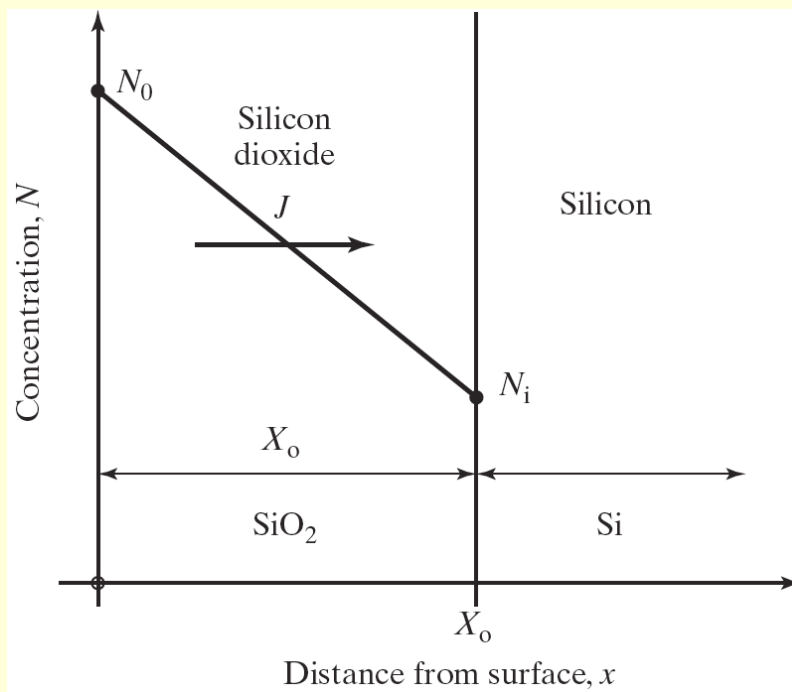
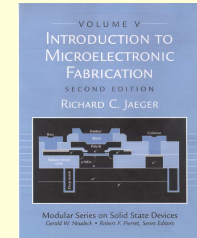
- Substitutional
- Interstitial

FIGURE 4.1

Atomic diffusion in a two-dimensional lattice. (a) Substitutional diffusion, in which the impurity moves among vacancies in the lattice; (b) interstitialcy mechanism, in which the impurity atom replaces a silicon atom in the lattice, and the silicon atom is displaced to an interstitial site; (c) interstitial diffusion, in which impurity atoms do not replace atoms in the crystal lattice.

Diffusion

Fick's First Law



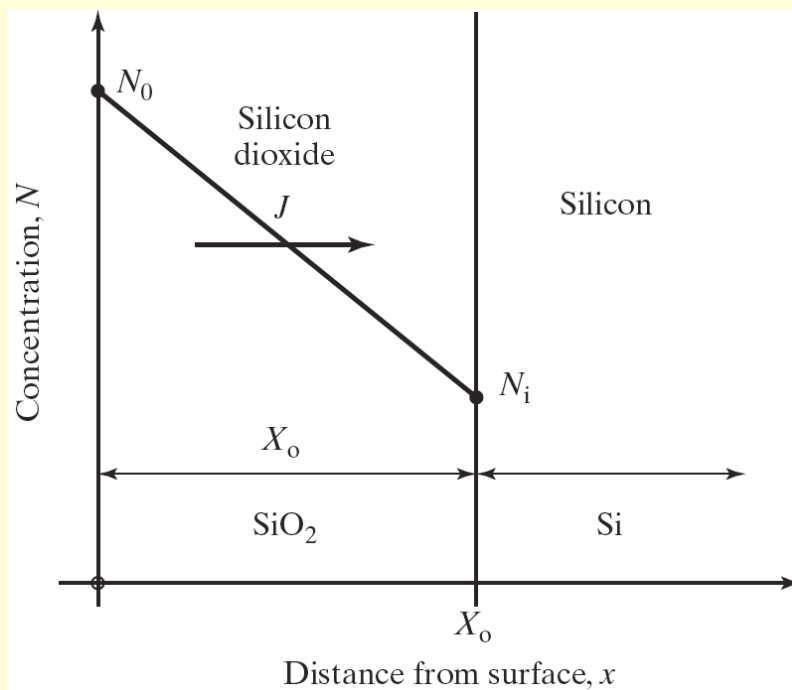
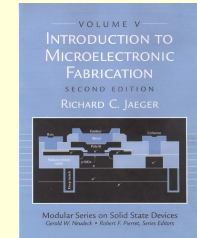
Particle flux J is proportional to the negative of the gradient of the particle concentration

$$J = -D \frac{\partial N}{\partial x}$$

D = diffusion coefficient

Diffusion

Fick's Second Law



Continuity Equation for Particle Flux :

Rate of increase of concentration is equal to the negative of the divergence of the particle flux

$$\frac{\partial N}{\partial t} = -\frac{\partial J}{\partial x}$$

(in one dimension)

Fick's Second Law of Diffusion :

Combine First Law with Continuity Eqn.

$$\frac{\partial N}{\partial t} = D \frac{\partial^2 N}{\partial x^2}$$

D assumed to be independent of concentration!

Constant Source Diffusion

Complementary Error Function Profiles

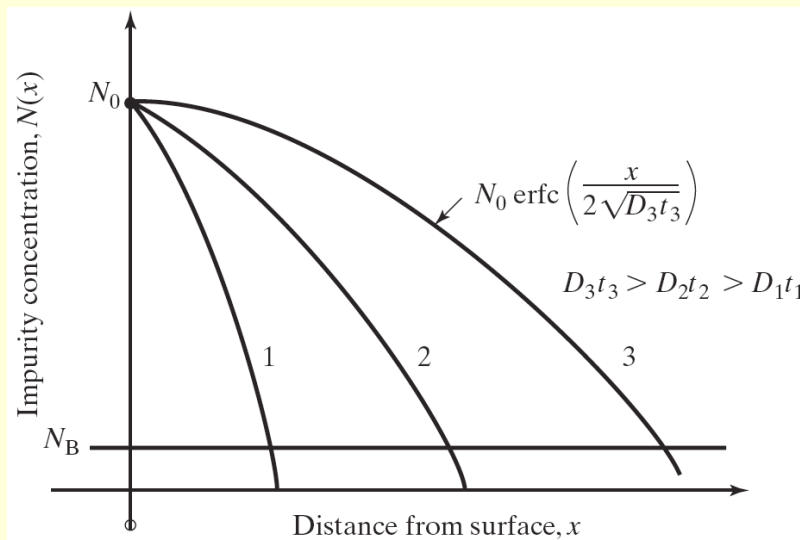
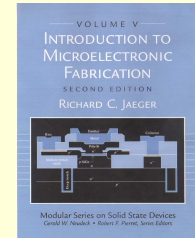


FIGURE 4.2

A constant-source diffusion results in a complementary error function impurity distribution. The surface concentration N_0 remains constant, and the diffusion moves deeper into the silicon wafer as the Dt product increases. Dt can change as a result of increasing diffusion time, increasing diffusion temperature, or a combination of both.

Concentration :
$$N(x, t) = N_0 \operatorname{erfc}\left(\frac{x}{2\sqrt{Dt}}\right)$$

Total Dose :
$$Q = \int_0^{\infty} N(x, t) dt = 2N_0 \sqrt{\frac{Dt}{\pi}}$$

N_0 = Surface Concentration

D = Diffusion Coefficient

erfc = Complementary Error Function

$$\operatorname{erfc}(z) = 1 - \operatorname{erf}(z)$$

$$\operatorname{erf}(z) = \frac{2}{\sqrt{\pi}} \int_0^z \exp[-x^2] dx$$

Limited Source Diffusion

Gaussian Profiles

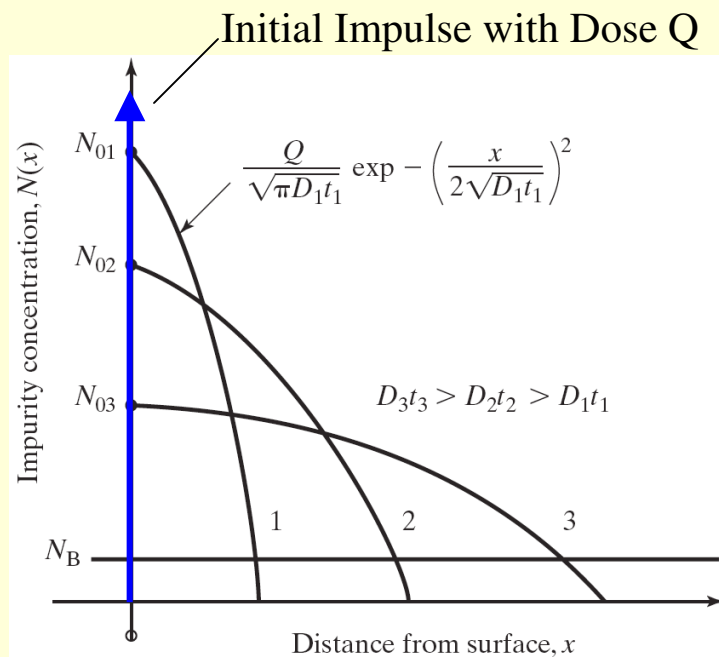
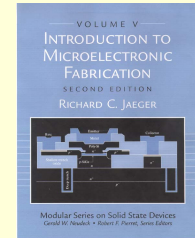


FIGURE 4.3

A Gaussian distribution results from a limited-source diffusion. As the Dt product increases, the diffusion front moves more deeply into the wafer, and the surface concentration decreases. The area (impurity dose) under each of the three curves is the same.

Concentration :

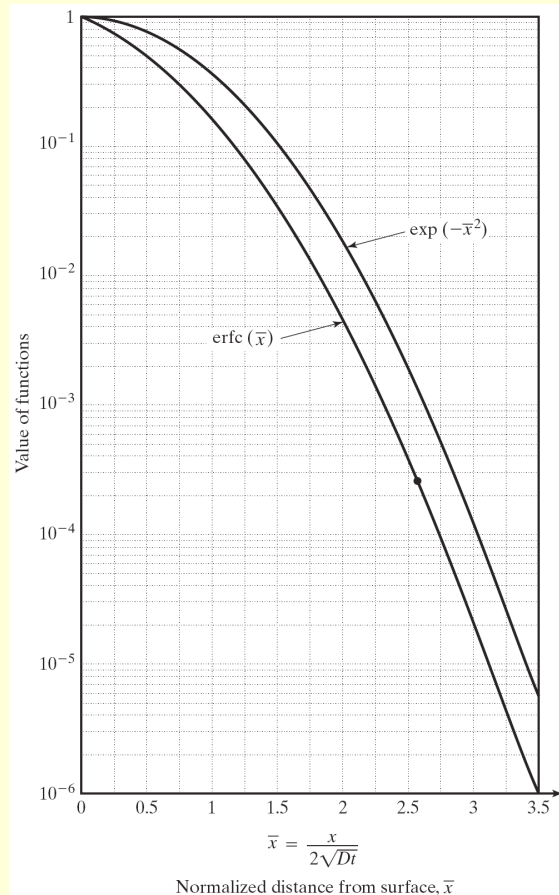
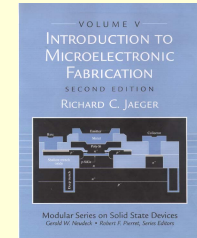
$$N(x, t) = N_0 \exp \left[- \left(\frac{x}{2\sqrt{Dt}} \right)^2 \right] = \frac{Q}{\sqrt{\pi Dt}} \exp \left[- \left(\frac{x}{2\sqrt{Dt}} \right)^2 \right]$$

$$N_0 = \text{Surface Concentration } N_0 = \frac{Q}{\sqrt{\pi Dt}}$$

D = Diffusion Coefficient

Gaussian Profile

Diffusion Profile Comparison



Complementary Error Function and
Gaussian Profiles are Similar in Shape

$$\text{erfc}(z) = 1 - \text{erf}(z)$$

$$\text{erf}(z) = \frac{2}{\sqrt{\pi}} \int_0^z \exp[-x^2] dx$$

FIGURE 4.4

A graph comparing the Gaussian and complementary error function (erfc) profiles. We use this curve to evaluate the erfc and its inverse.

Diffusion Coefficients

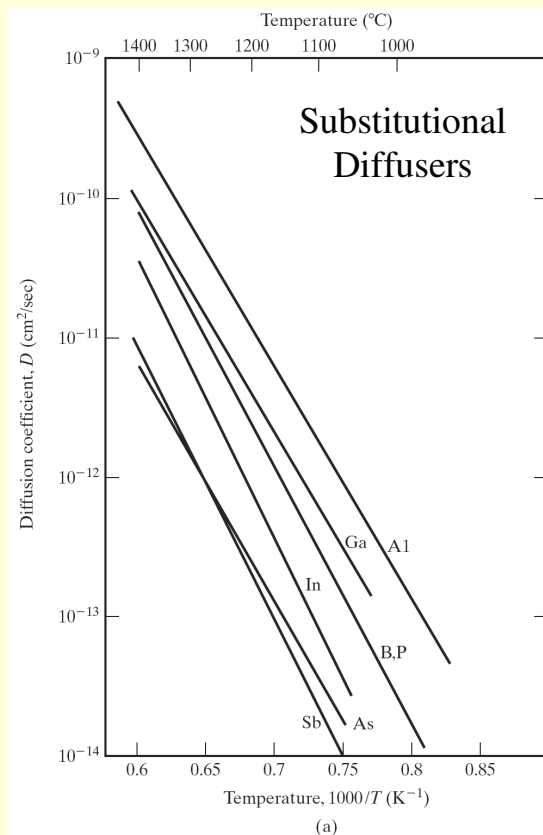
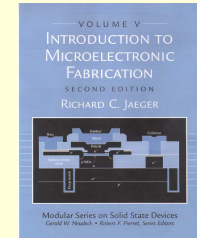
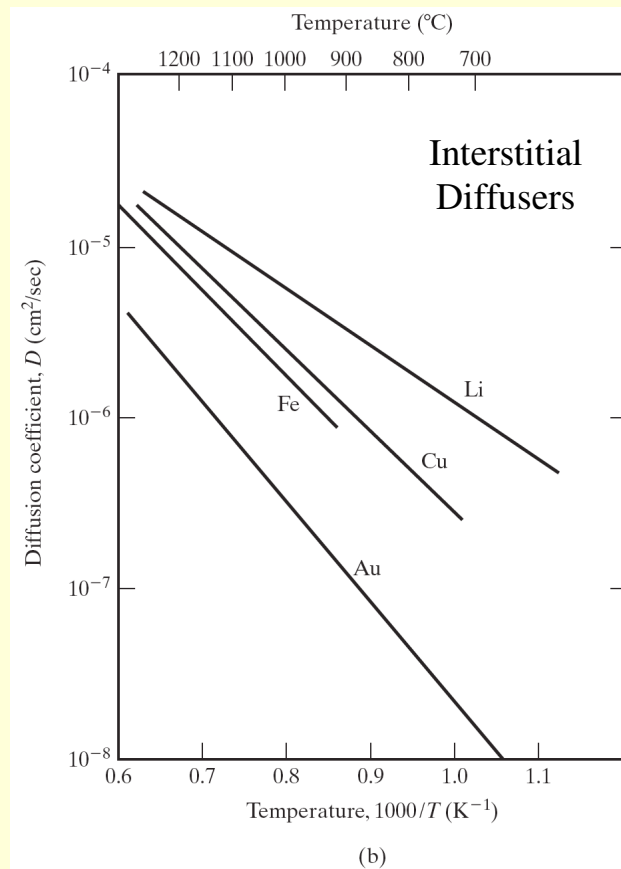
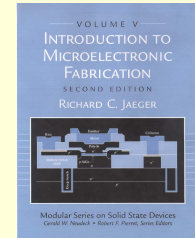


FIGURE 4.5

Diffusion constants in silicon for (a) substitutional diffusers (above) and (b) interstitial diffusers (next page). Copyright John Wiley & Sons, Inc.; reprinted with permission from Ref. [28].



Diffusion Coefficients



$$D = D_o \exp\left(-\frac{E_A}{kT}\right) \quad \text{Arrhenius Relationship}$$

E_A = activation energy

k = Boltzmann's constant = 1.38×10^{-23} J/K

T = absolute temperature

TABLE 4.1 Typical Diffusion Coefficient Values for a Number of Impurities.

Element	D_o (cm ² /sec)	E_A (eV)
B	10.5	3.69
Al	8.00	3.47
Ga	3.60	3.51
In	16.5	3.90
P	10.5	3.69
As	0.32	3.56
Sb	5.60	3.95

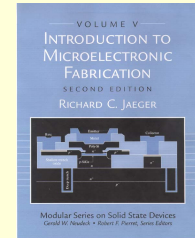
Example 4.1

Calculate the diffusion coefficient for boron at 1100 °C.

Solution: From Table 4.1, $D_o = 10.5$ cm²/sec and $E_A = 3.69$ eV. $T = 1373$ K.

$$D = 10.5 \exp - \frac{3.69}{(8.614 \times 10^{-5})(1373)} = 2.96 \times 10^{-13} \text{cm}^2/\text{sec}.$$

Successive Diffusions

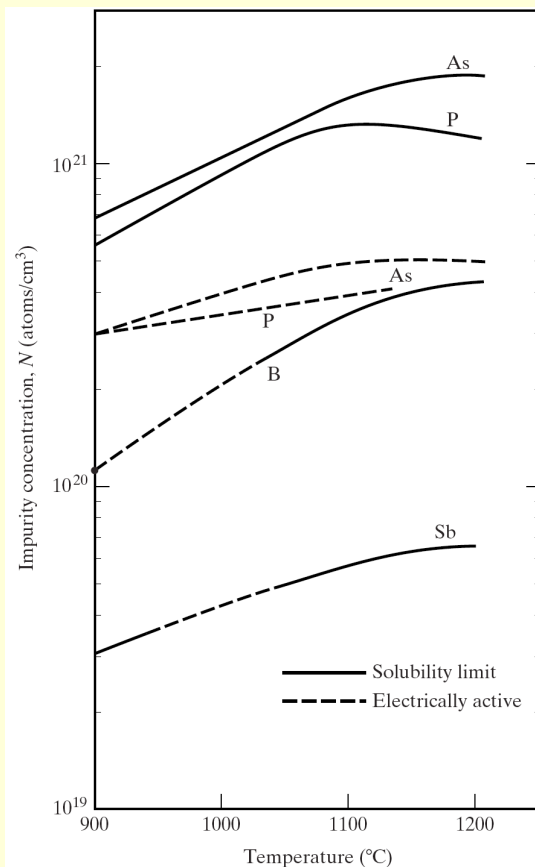
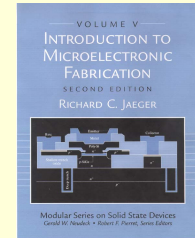


- Successive Diffusions Using Different Times and Temperatures
- Final Result Depends Upon the Total Dt Product

$$(Dt)_{tot} = \sum_i D_i t_i$$

Diffusion

Solid Solubility Limits



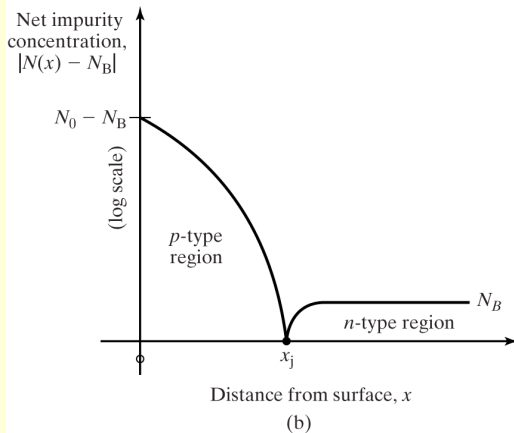
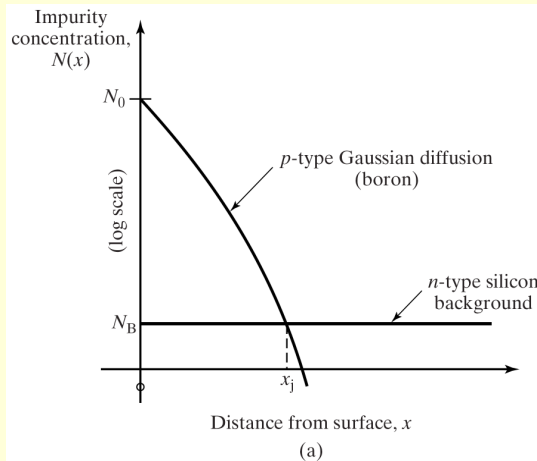
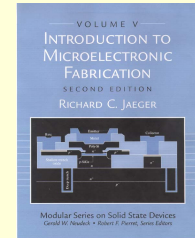
- There is a limit to the amount of a given impurity that can be “dissolved” in silicon (the Solid Solubility Limit)
- At high concentrations, all of the impurities introduced into silicon will not be electrically active

FIGURE 4.6

The solid-solubility and electrically active impurity-concentration limits in silicon for antimony, arsenic, boron, and phosphorus. Reprinted with permission from Ref. [29]. This paper was originally presented at the 1977 Spring Meeting of The Electrochemical Society, Inc., held in Philadelphia, Pennsylvania.

Diffusion

p-n Junction Formation



x_j = Metallurgical Junction Depth

P - n junction occurs at the point x_j where the net impurity concentration is zero

(i. e. p - type doping cancels out n - type doping)

Gaussian Profile :
$$x_j = 2\sqrt{Dt \ln\left(\frac{N_0}{N_B}\right)}$$

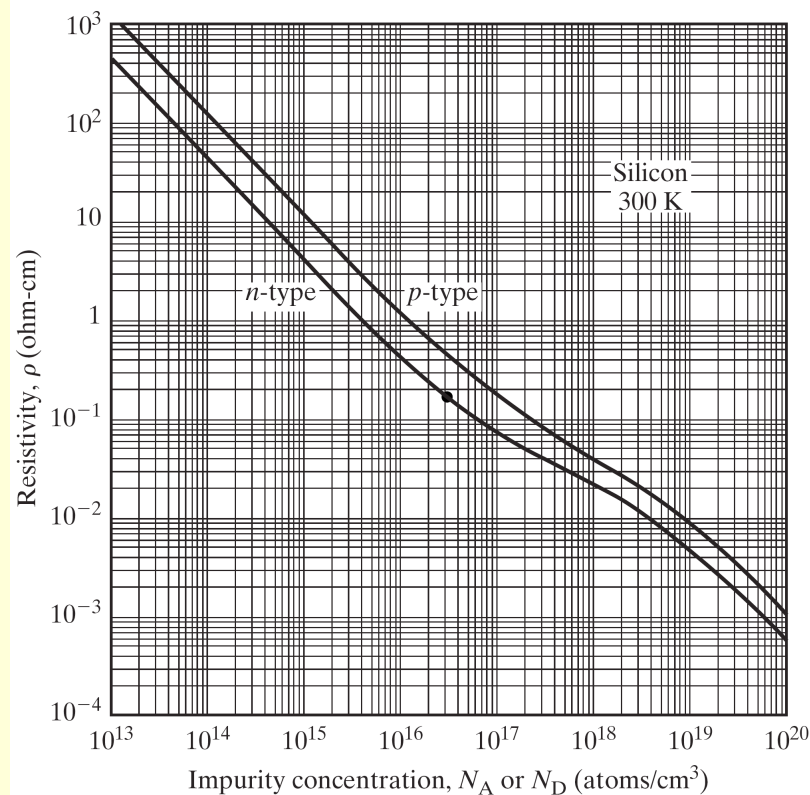
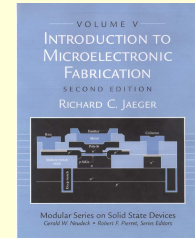
Error Function profile :
$$x_j = 2\sqrt{Dt} \operatorname{erfc}^{-1}\left(\frac{N_0}{N_B}\right)$$

FIGURE 4.7

Formation of a pn junction by diffusion. (a) An example of a p -type Gaussian diffusion into a uniformly doped n -type wafer; (b) net impurity concentration in the wafer. The metallurgical junction occurs at the point $x = x_j$ where the net concentration is zero. The material is converted to p -type to the left of x_j and remains n -type to the right of x_j .

Diffusion

Resistivity vs. Doping



$$\rho = \sigma^{-1} = [q(\mu_n n + \mu_p p)]^{-1}$$

$$n\text{-type} : \rho \cong [q\mu_n (N_D - N_A)]^{-1}$$

$$p\text{-type} : \rho \cong [q\mu_p (N_A - N_D)]^{-1}$$

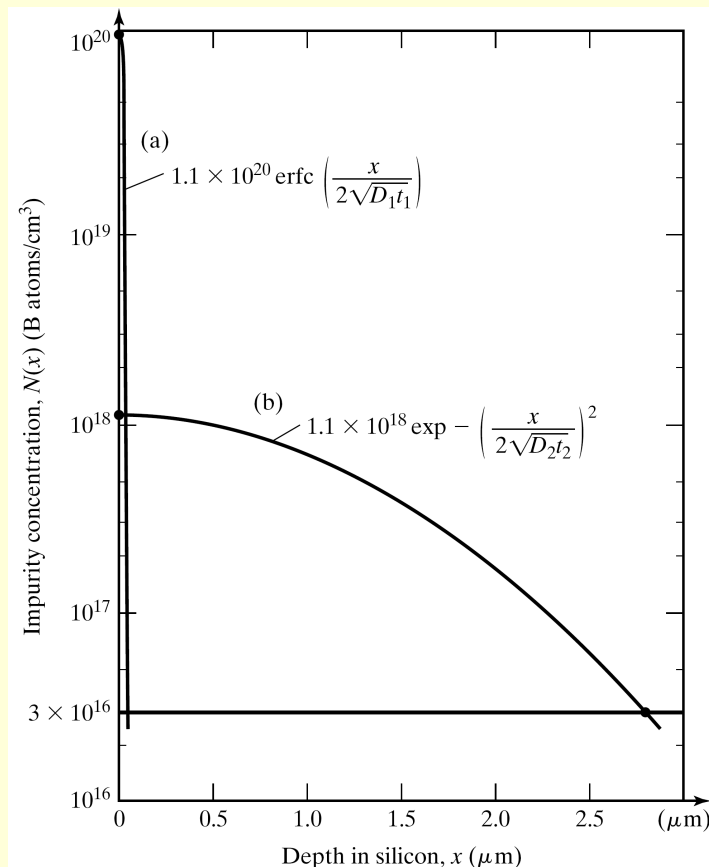
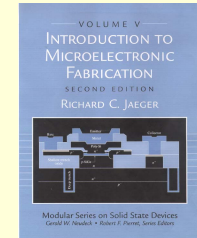
FIGURE 4.8

Room-temperature resistivity in n - and p -type silicon as a function of impurity concentration. (Note that these curves are valid for either donor or acceptor impurities but not for compensated material containing both types of impurities.)

Copyright 1987 Addison-Wesley Publishing Company. Reprinted with permission from Ref. [3].

Diffusion

Two Step Diffusion



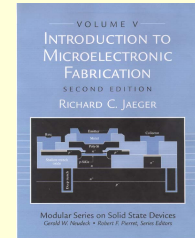
- Short constant source diffusion used to establish dose Q (“Predep” step)
- Longer limited source diffusion drives profile in to desired depth (“drive in” step)
- Final profile is Gaussian

FIGURE 4.9

Calculated boron impurity profiles for Example 4.2. (a) Following the predeposition step at 900°C for 15 min; (b) following a subsequent 5-hr drive-in step at $1,100^{\circ}\text{C}$. The final junction depth is $2.77\text{ }\mu\text{m}$ with a surface concentration of $1.1 \times 10^{18}/\text{cm}^3$. The initial profile approximates an impulse.

Diffusion Calculation

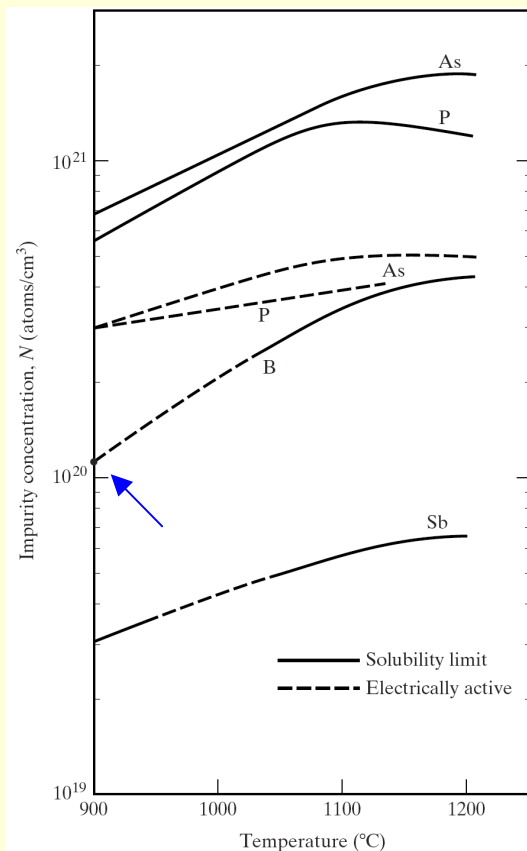
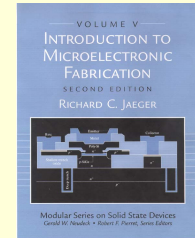
Example 4.3 - Boron Diffusion



- A boron diffusion is used to form the base region of an npn transistor in a $0.18\ \Omega\text{-cm}$ n-type silicon wafer. A solid-solubility-limited boron predeposition is performed at 900°C for 15 min followed by a 5-hr drive-in at 1100°C . Find the surface concentration and junction depth (a) after the predep step and (b) after the drive-in step.

Diffusion Calculation

Example 4.3 - Boron Diffusion



Predeposition step is solid-solubility limited.

$$T_1 = 900^\circ\text{C} = 1173\text{K} \rightarrow N_o = 1.1 \times 10^{20} / \text{cm}^3$$

$$D_1 = 10.5 \exp \left[-\frac{3.69\text{eV}}{(8.614 \times 10^{-5} \text{eV/K}) 1173\text{K}} \right] = 1.45 \times 10^{-15} \text{cm}^2 / \text{sec}$$

$$t_1 = 15 \text{ min} = 900 \text{ sec} \quad D_1 t_1 = 1.31 \times 10^{-12} \text{cm}^2$$

$$N(x) = 1.1 \times 10^{20} \operatorname{erfc} \left(\frac{x}{2.28 \times 10^{-6} \text{cm}} \right) / \text{cm}^3$$

$$\text{Dose: } Q = 2N_o \sqrt{\frac{D_1 t_1}{\pi}} = 1.42 \times 10^{14} / \text{cm}^2$$

$$T_2 = 1100^\circ\text{C} = 1373\text{K}$$

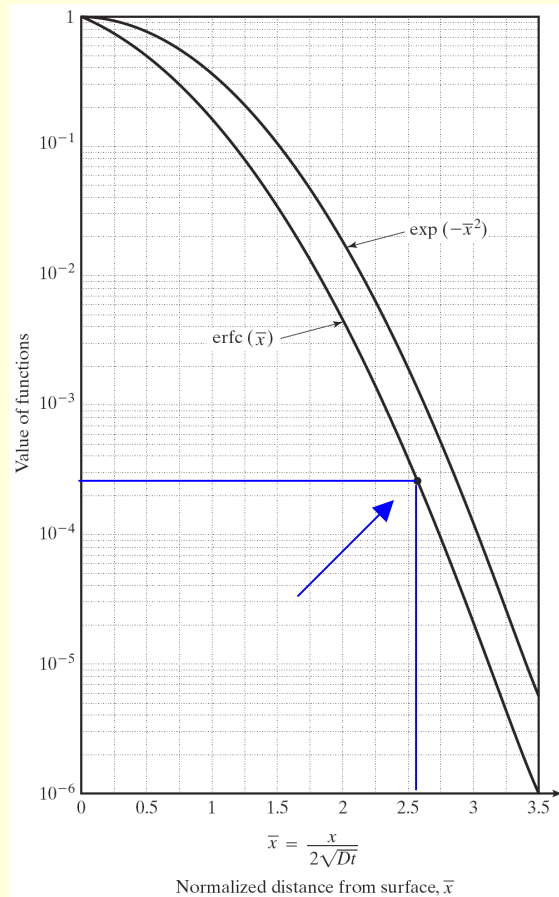
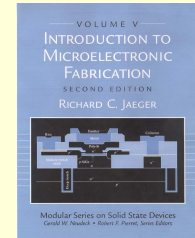
$$D_2 = 10.5 \exp \left[-\frac{3.69\text{eV}}{(8.614 \times 10^{-5} \text{eV/K}) 1373\text{K}} \right] = 2.96 \times 10^{-13} \text{cm}^2 / \text{sec}$$

$$t_2 = 5 \text{ hr} = 18000 \text{ sec} \quad D_2 t_2 = 5.33 \times 10^{-9} \text{cm}^2$$

$$N_2(x) = \frac{1.42 \times 10^{14} / \text{cm}^2}{\sqrt{\pi(5.33 \times 10^{-9} \text{cm}^2)}} \exp \left(-\frac{x^2}{2\sqrt{D_2 t_2}} \right) = 1.1 \times 10^{18} \exp \left(-\frac{x^2}{1.46 \times 10^{-4}} \right) / \text{cm}^3$$

Diffusion Calculation

Example 4.3 (cont.)



$$N_1(x) = 1.1 \times 10^{20} \operatorname{erfc}\left(\frac{x}{2.28 \times 10^{-6} \text{ cm}}\right) / \text{cm}^3$$

$$x_{j1} = 2\sqrt{D_1 t_1} \operatorname{erfc}^{-1}\left(\frac{N_o}{N_B}\right) = (2.28 \times 10^{-6} \text{ cm}) \operatorname{erfc}^{-1}\left(\frac{3 \times 10^{16}}{1.1 \times 10^{20}}\right) = (2.28 \times 10^{-6} \text{ cm}) \operatorname{erfc}^{-1}(2.73 \times 10^{-4})$$

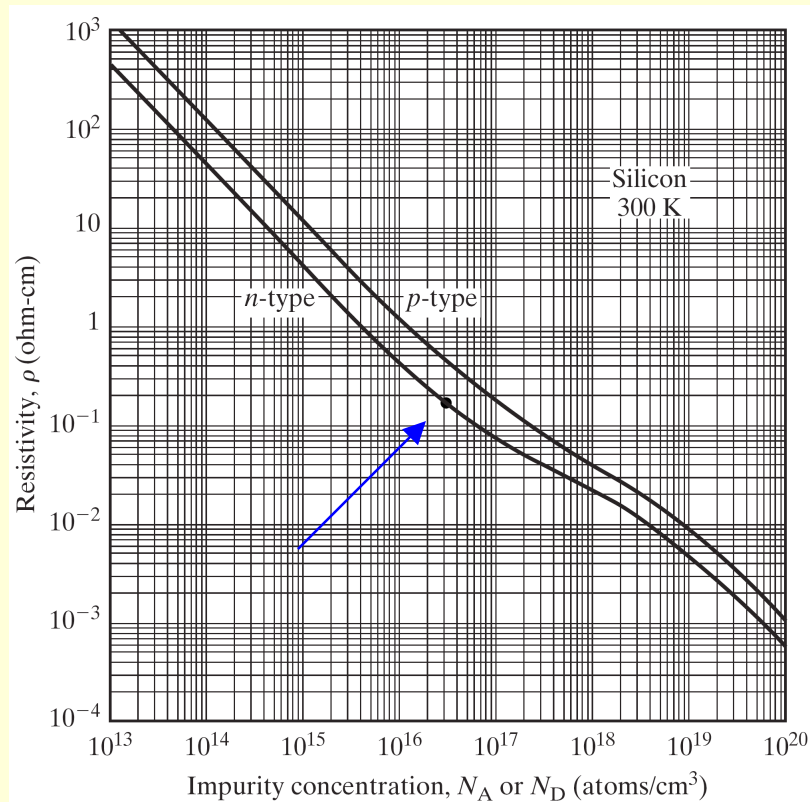
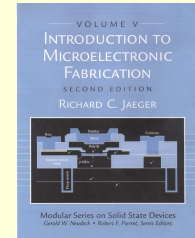
$$x_{j1} = (2.28 \times 10^{-6} \text{ cm})(2.57) = 5.86 \times 10^{-6} \text{ cm} = 0.058 \mu\text{m}$$

$$N_2(x) = 1.1 \times 10^{18} \exp\left(-\frac{x^2}{1.46 \times 10^{-4} \text{ cm}^2}\right) / \text{cm}^3$$

$$x_{j2} = 1.46 \times 10^{-4} \text{ cm} \sqrt{\ln\left(\frac{1.1 \times 10^{18}}{3 \times 10^{16}}\right)} = 2.77 \times 10^{-4} \text{ cm} = 2.77 \mu\text{m}$$

Diffusion Calculation

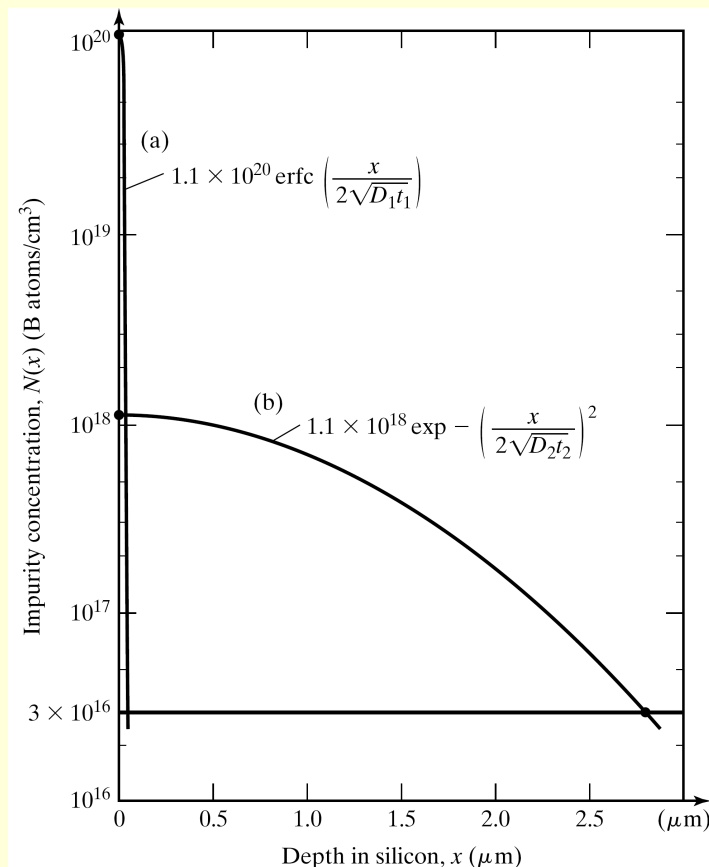
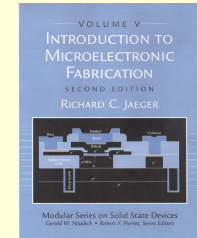
Example 4.3 (cont.)



Starting Wafer : n - type $0.18 \, \Omega\text{-cm}$

n - type $0.18 \, \Omega\text{-cm} \rightarrow N_D = 3 \times 10^{16}/\text{cm}^3$

Two Step Diffusion

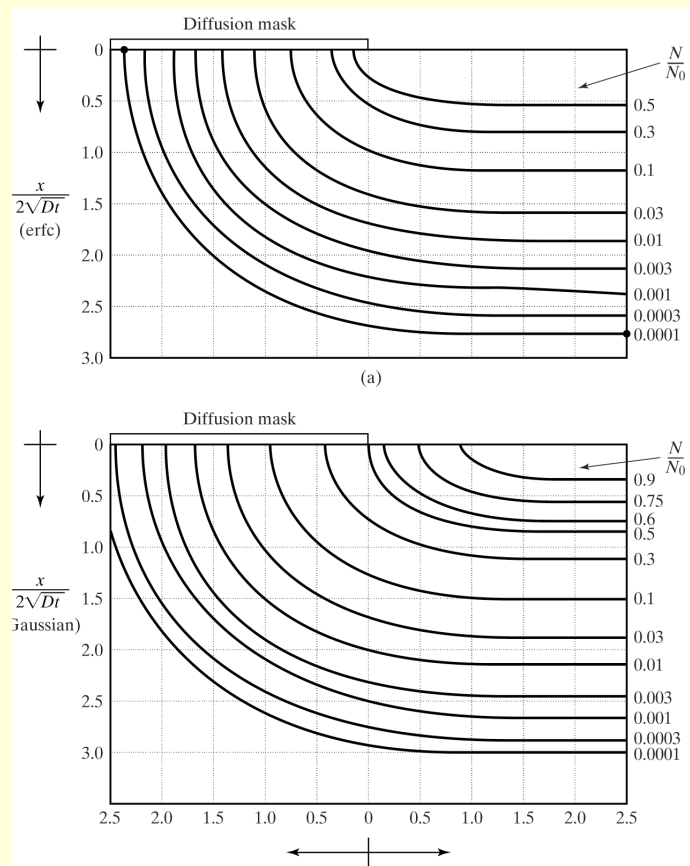
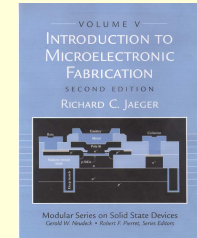


- Short constant source diffusion used to establish dose Q (“Predep” step)
- Longer limited source diffusion drives profile in to desired depth (“drive in” step)
- Final profile is Gaussian

FIGURE 4.9

Calculated boron impurity profiles for Example 4.2. (a) Following the predeposition step at 900°C for 15 min; (b) following a subsequent 5-hr drive-in step at $1,100^{\circ}\text{C}$. The final junction depth is $2.77\text{ }\mu\text{m}$ with a surface concentration of $1.1 \times 10^{18}/\text{cm}^3$. The initial profile approximates an impulse.

Lateral Diffusion Under Mask Edge



- Diffusion is really a 3-D process. As impurities diffuse vertically, they also diffuse horizontally in both directions.
- Diffusion proceeds laterally under the edge of the mask opening

FIGURE 4.10

Normalized two-dimensional complementary error function and Gaussian diffusions near the edge of a window in the barrier layer. Copyright 1965 by International Business Machines Corporation; reprinted with permission from Ref. [4].

Lateral Diffusion Under Mask Edge

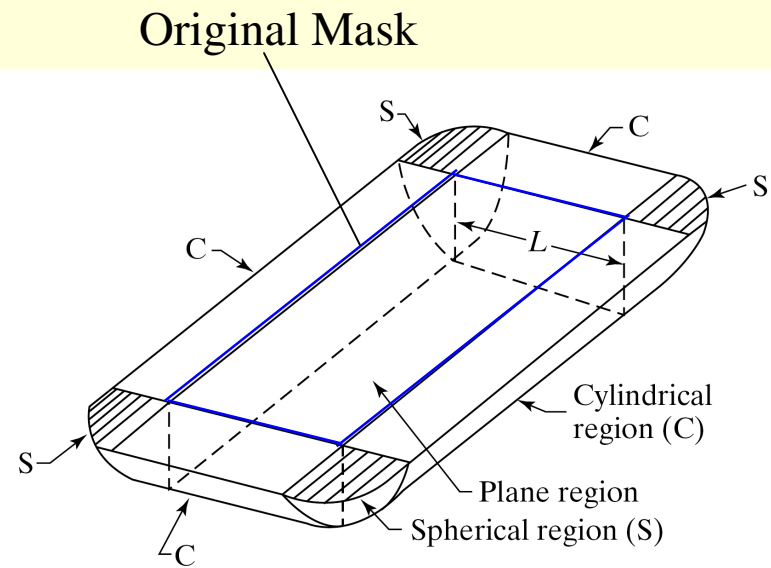
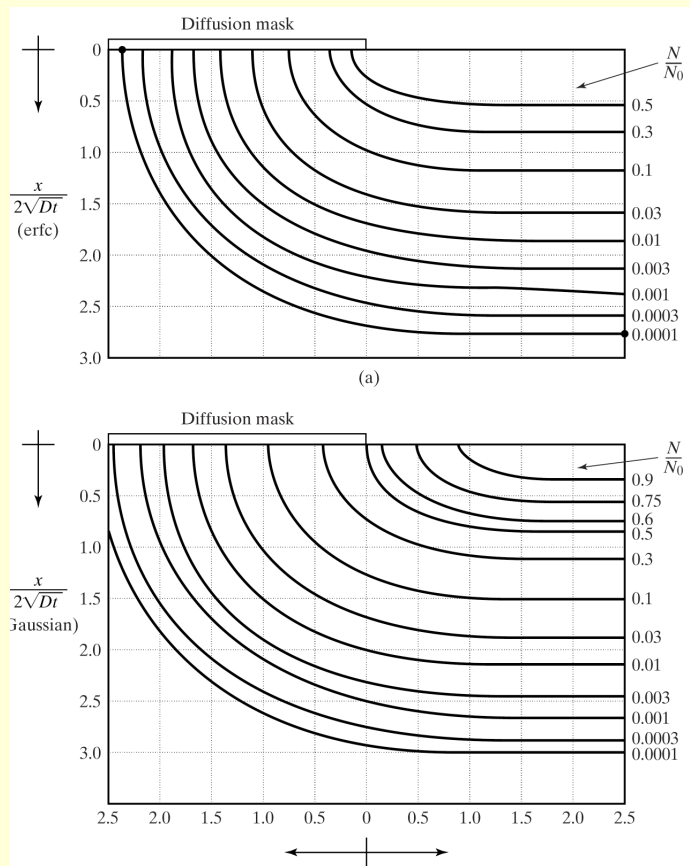
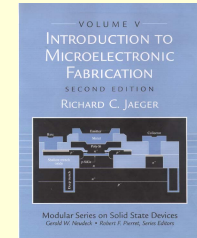


FIGURE 4.10

Normalized two-dimensional complementary error function and Gaussian diffusions near the edge of a window in the barrier layer. Copyright 1965 by International Business Machines Corporation; reprinted with permission from Ref. [4].

Concentration Dependent Diffusion

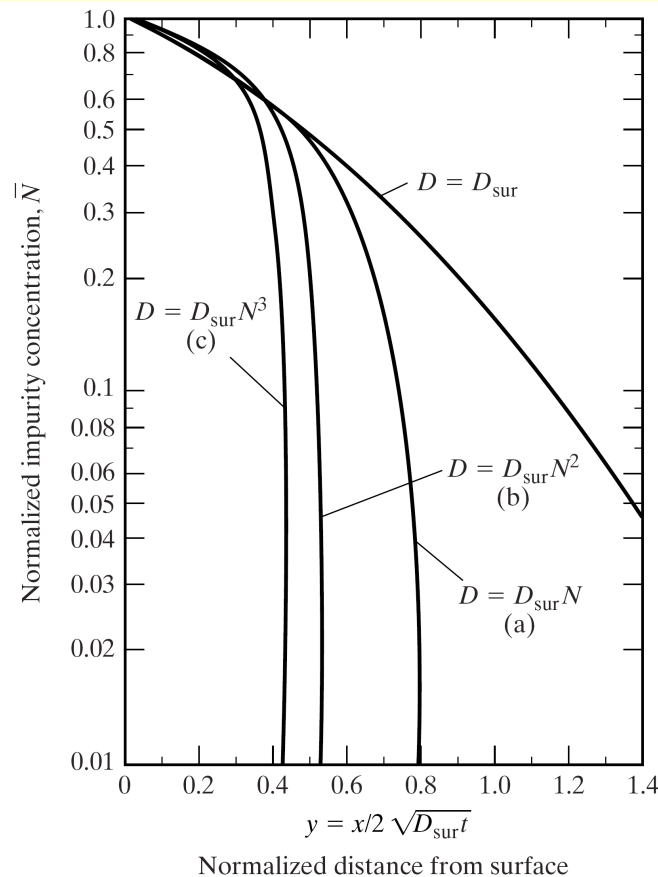
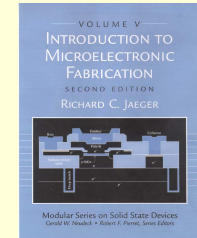


TABLE 4.2 Properties of High-Concentration Arsenic and Boron Diffusions

Element	$x_j(\text{cm})$	$D(\text{cm}^2/\text{sec})$	$N_0(\text{cm}^{-3})$	$Q(\text{cm}^{-2})$
Arsenic	$2.29\sqrt{N_0 D t / n_i^*}$	$22.9 \exp(-4.1/kT)$	$1.56 \times 10^{17} (R_s x_j)^{-1}$	$0.55 N_0 x_j$
Boron	$2.45\sqrt{N_0 D t / n_i^*}$	$3.17 \exp(-3.59/kT)$	$2.78 \times 10^{17} (R_s x_j)^{-1}$	$0.67 N_0 x_j$

Second Law of Diffusion

$$\frac{\partial N}{\partial t} = \frac{\partial}{\partial x} D(x) \frac{\partial N}{\partial x}$$

Profiles More Abrupt at High Concentrations

FIGURE 4.11

Diffusion profiles for concentration-dependent diffusion. Copyright 1963 by the American Physical Society. Reprinted with permission from Ref. [6].

Concentration Dependent Diffusion

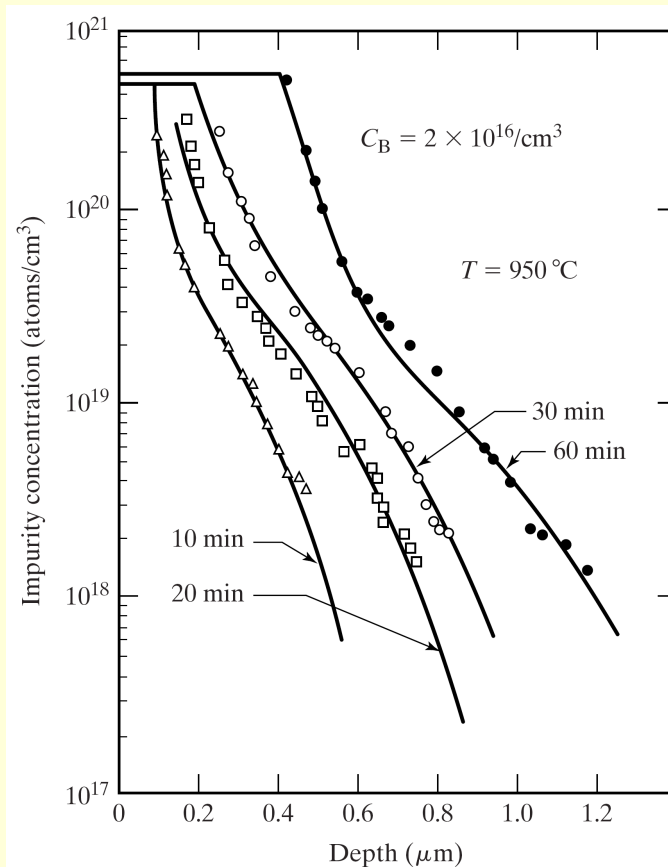
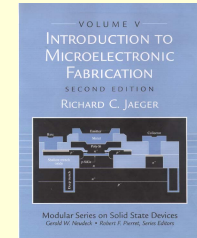


FIGURE 4.12

Shallow phosphorus diffusion profiles for constant-source diffusions at 950 °C. Copyright 1969 IEEE. Reprinted with permission from Ref. [10].

Resistors

Sheet Resistance

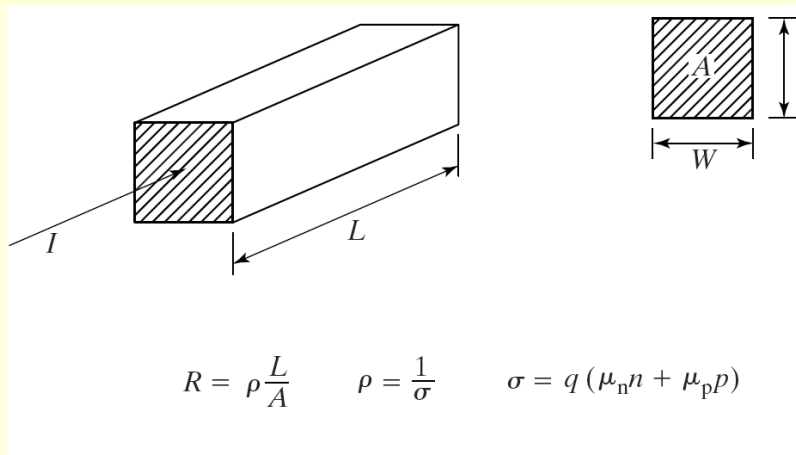
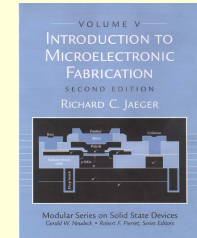


FIGURE 4.13

Resistance of a block of material having uniform resistivity. A uniform current distribution is entering the material perpendicular to the end of the block. The ratio of resistivity to thickness is called the *sheet resistance* of the material.

$$A = W \cdot t$$

$$R = \left(\frac{\rho}{t} \right) \left(\frac{L}{W} \right) = R_s \left(\frac{L}{W} \right)$$

$$R_s = \frac{\rho}{t} = \text{Sheet Resistance [Ohms per Square]}$$

$$\left(\frac{L}{W} \right) = \text{Number of Squares of Material}$$

Resistors

Counting Squares

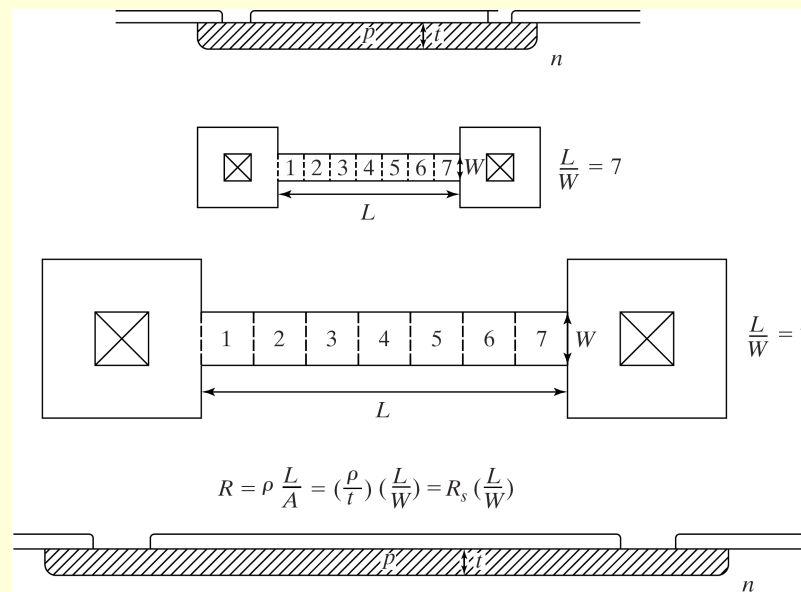
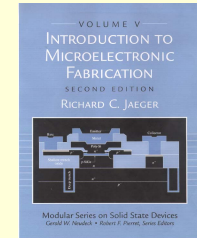


Figure 4.14

- Top and Side Views of Two Resistors of Different Size
- Resistors Have Same Value of Resistance
- Each Resistor is 7 \square in Length
- Each End Contributes Approximately 0.65 \square
- Total for Each is 8.3 \square

Resistors

Contact and Corner Contributions

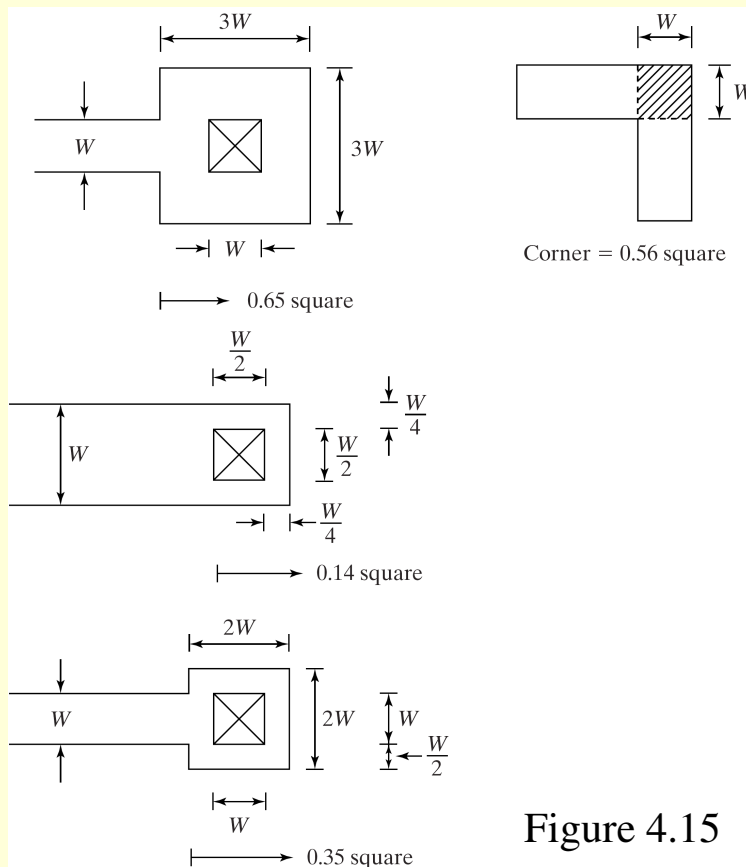
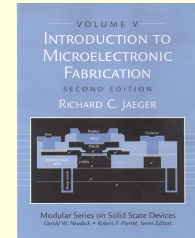
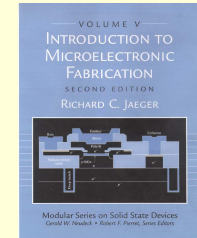


Figure 4.15

- Effective Square Contributions of Various Resistor End and Corner Configurations

Sheet Resistance

Irvin's Curves



$$\bar{\rho} = \frac{1}{\sigma} = \frac{1}{\frac{1}{x_j} \int_0^{x_j} \sigma(x) dx}$$

$$R_s = \frac{\bar{\rho}}{x_j} = \frac{1}{\int_0^{x_j} \sigma(x) dx}$$

$$R_s \cong \left[\int_0^{x_j} q\mu N(x) dx \right]^{-1}$$

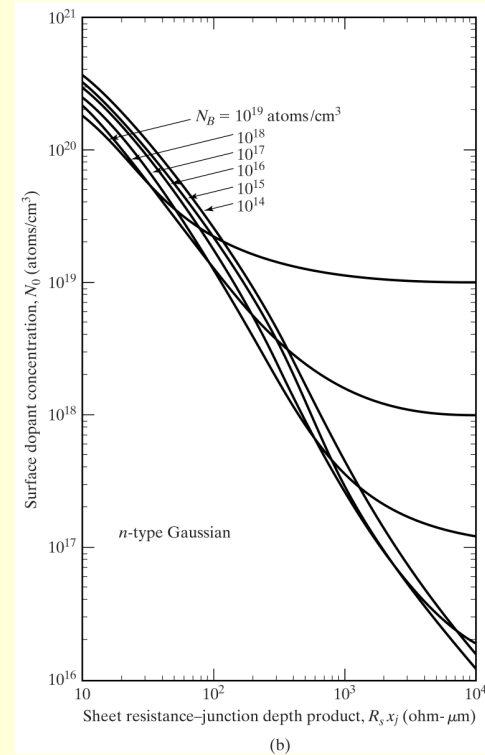
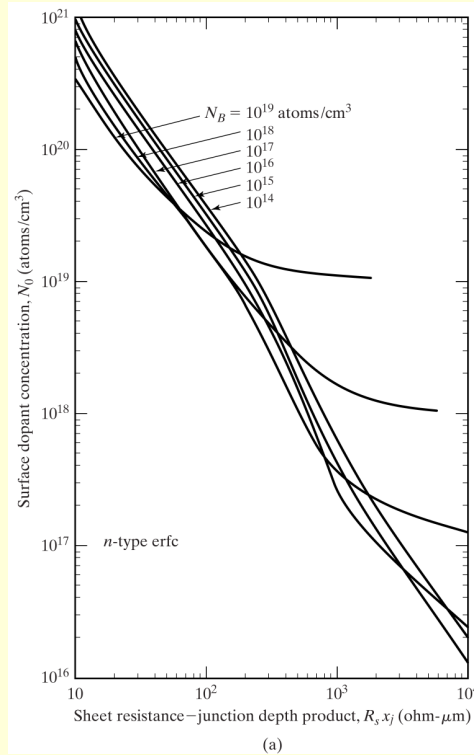
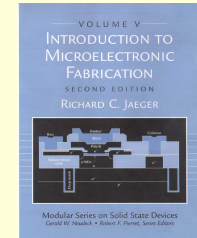
- Irvin Evaluated this Integral and Published a Set of Normalized Curves Plot Surface Concentration Versus Average Resistivity

$$\bar{\rho} = R_s x_j$$

- Four Sets of Curves
 - n-type and p-type
 - Gaussian and erfc

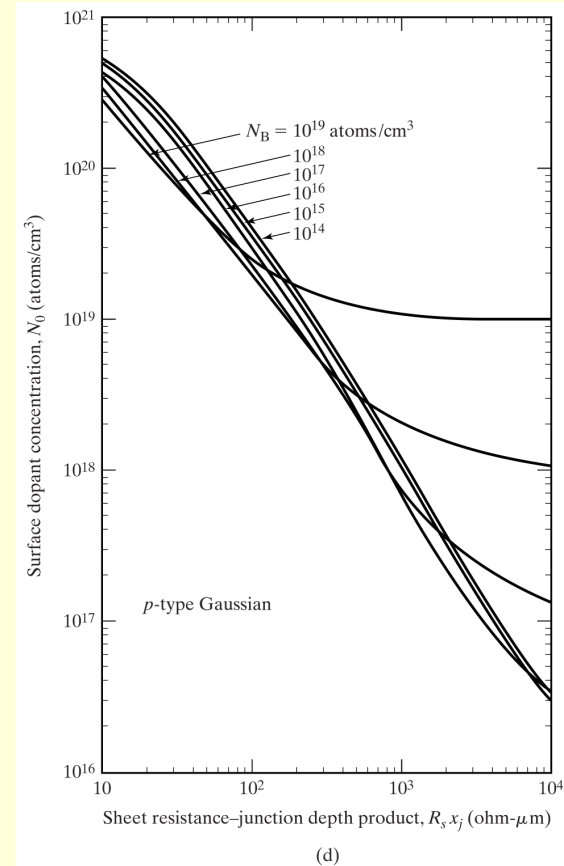
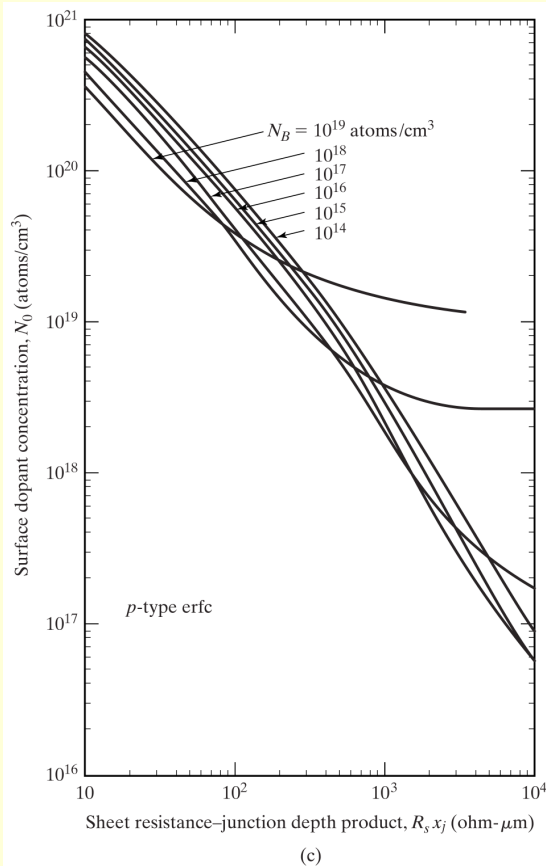
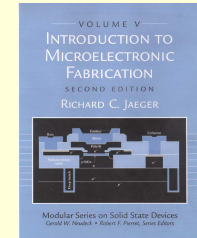
Sheet Resistance

Irvin's Curves



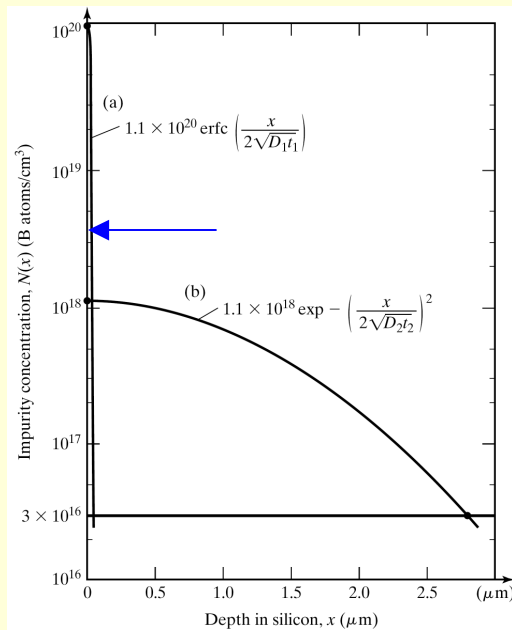
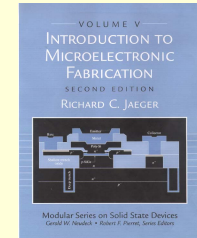
Sheet Resistance

Irvin's Curves (cont.)



Two Step Diffusion

Sheet Resistance - Predep Step



Initial Profile

$$N_o = 1.1 \times 10^{20} / \text{cm}^3$$

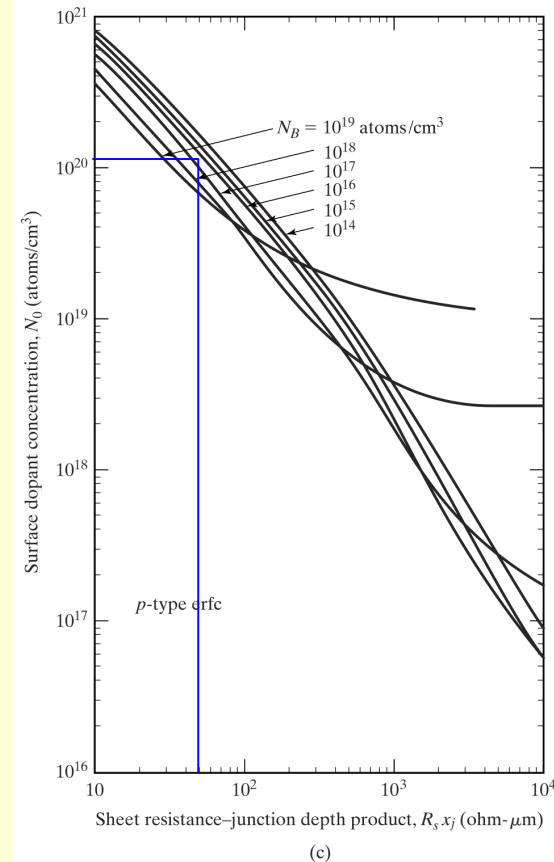
$$N_B = 3 \times 10^{16} / \text{cm}^3$$

$$x_j = 0.0587 \mu\text{m}$$

p-type erfc profile

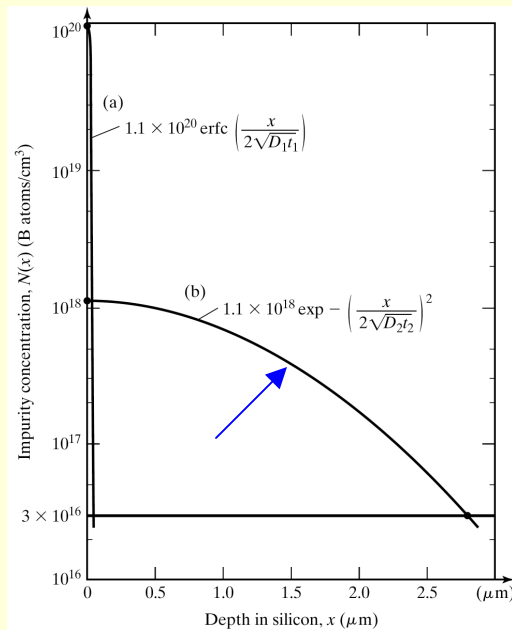
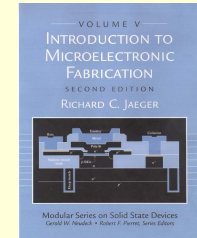
$$R_s x_j = 50 \Omega - \mu\text{m}$$

$$R_s = \frac{32 \Omega - \mu\text{m}}{0.0587 \mu\text{m}} = 850 \Omega/\text{Square}$$



Two Step Diffusion

Sheet Resistance - Drive-in Step



Final Profile

$$N_o = 1.1 \times 10^{18} / \text{cm}^3$$

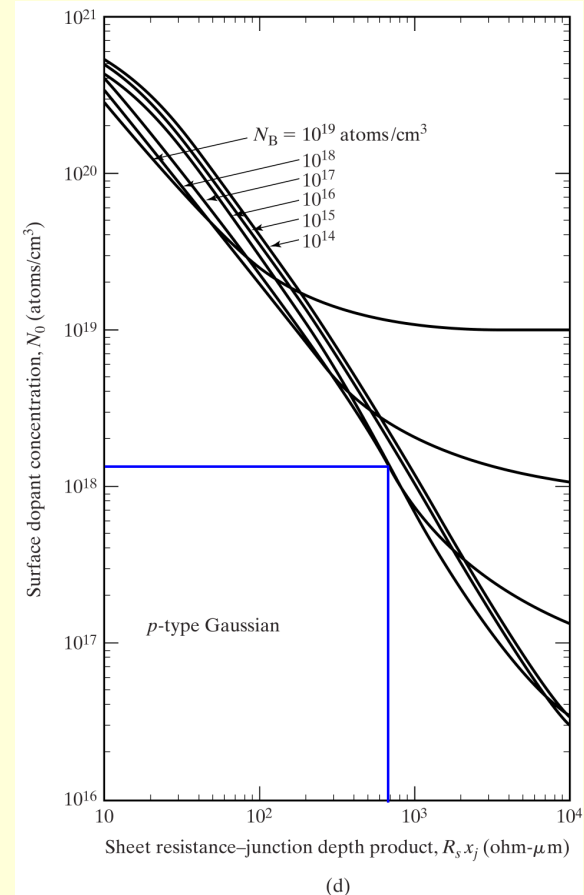
$$N_B = 3 \times 10^{16} / \text{cm}^3$$

$$x_j = 2.73 \mu\text{m}$$

p-type Gaussian profile

$$R_s x_j = 700 \Omega - \mu\text{m}$$

$$R_s = \frac{700 \Omega - \mu\text{m}}{2.73 \mu\text{m}} = 260 \Omega/\text{Square}$$



Resistivity Measurement

Four-Point Probe

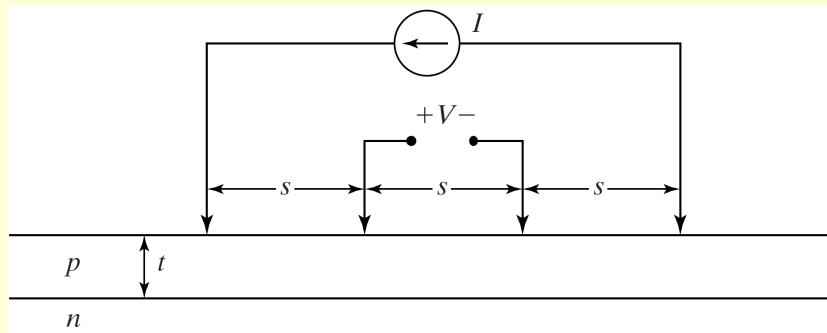
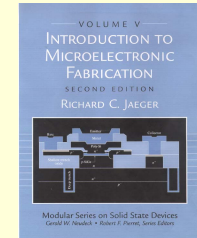


FIGURE 4.17

Four-point probe with probe spacing s used for direct measurement of bulk wafer resistivity and the sheet resistance of thin diffused layers. A known current is forced through the outer probes, and the voltage developed is measured across the inner probes. (See Eqs. (4.16) through (4.18).)

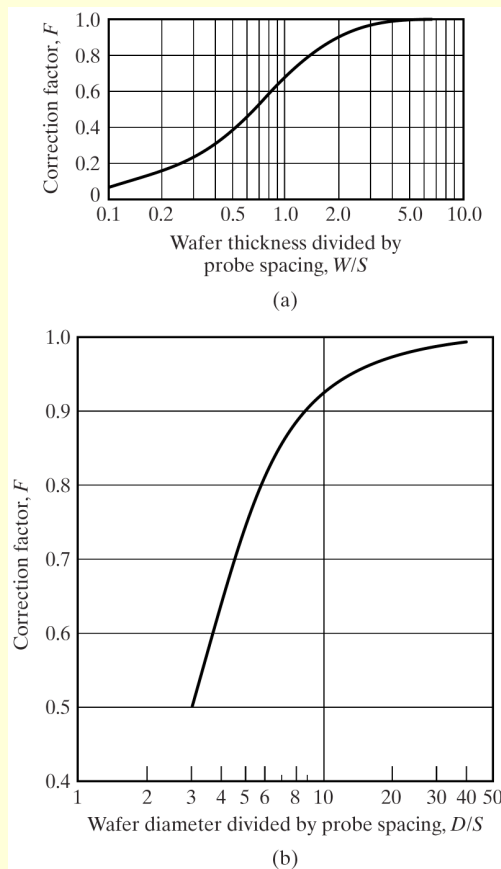
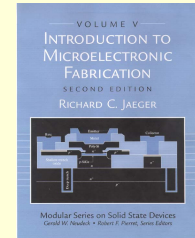
$$\rho = 2\pi s \frac{V}{I} \quad [\Omega \cdot \text{m}] \quad \text{for } t \gg s$$

$$\rho = \frac{\pi t}{\ln 2} \frac{V}{I} \quad [\Omega \cdot \text{m}] \quad \text{for } s \gg t$$

$$R_s = \frac{\rho}{t} = \frac{\pi}{\ln 2} \frac{V}{I} \cong 4.53 \frac{V}{I} \quad [\Omega/\text{square}]$$

Four Terminal Resistance Measurement

Four-Point Probe Correction Factors



Correction Factors

(a) Wafers Thick Relative to the Probe Spacing

(b) Wafers of Finite Diameter

$$\rho = F \rho_{\text{measured}}$$

FIGURE 4.18

Four-point-probe correction factors, F , used to correct for (a) wafers which are relatively thick compared to the probe spacing s and (b) wafers of finite diameter. In each case $\text{---} = F_{\text{measured}}$. (a) Copyright 1975 by McGraw-Hill Book Company. Reprinted with permission from Ref. [12]. (b) Reprinted from Ref. [30] with permission from the AT&T Technical Journal. Copyright 1958 AT&T.

Sheet Resistance van der Pauw's Method

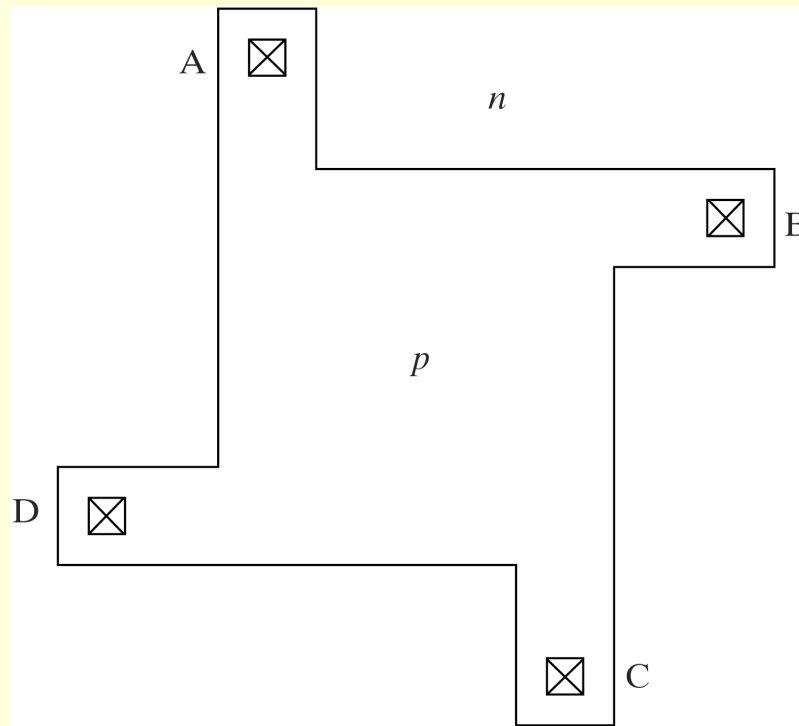
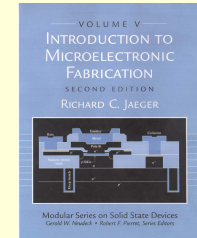


FIGURE 4.19

A simple van der Pauw test structure used to measure the sheet resistance of a diffused layer. Sheet resistance is calculated using Eq. (4.20).

Van der Pauw's Theory

Any Four - Terminal Region without Holes

$$\exp\left(-\pi \frac{R_{AB,CD}}{\rho}\right) + \exp\left(-\pi \frac{R_{BC,DA}}{\rho}\right) = 1$$

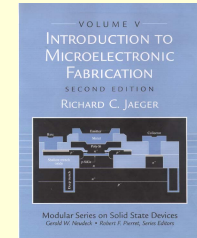
$$R_{AB,CD} = \frac{V_{CD}}{I_{AB}} \quad \text{and} \quad R_{BC,DA} = \frac{V_{DA}}{I_{BC}}$$

For symmetrical structure $R_{AB,CD} = R_{AB,CD}$

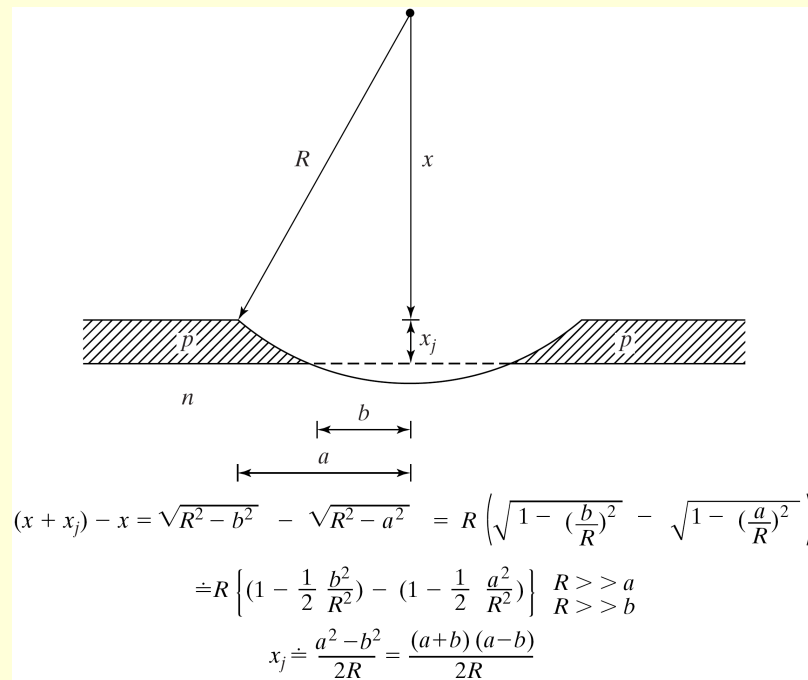
$$R_s = \frac{\rho}{t} = \left(\frac{\pi}{\ln 2}\right) \frac{V_{CD}}{I_{AB}}$$

Four Terminal Resistance Measurement

Junction Depth Measurement



- Groove and Stain Method

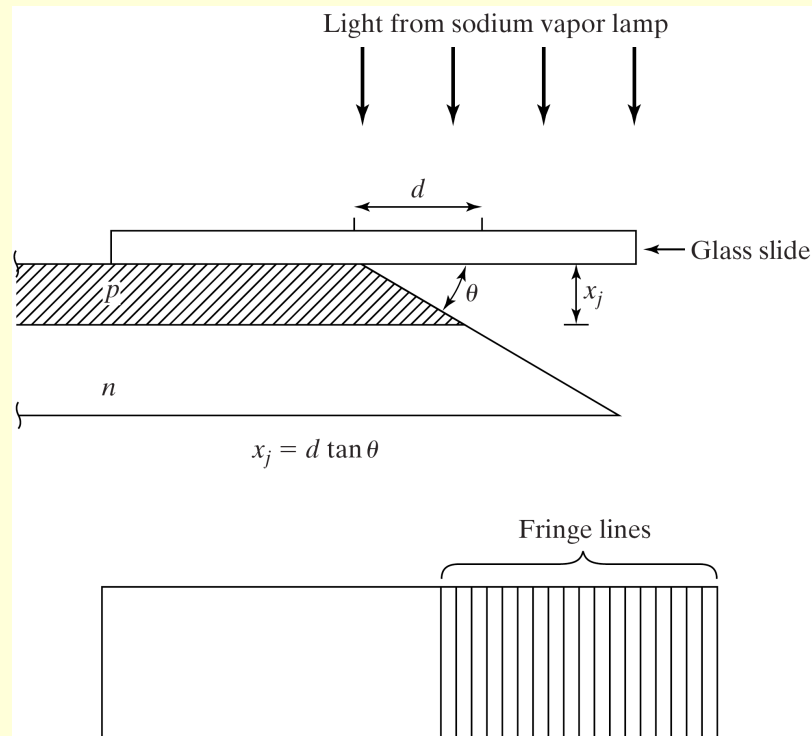
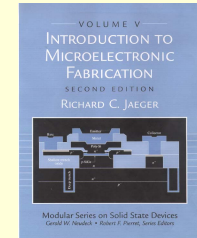


$$x_j = \frac{(a+b)(a-b)}{2R}$$

FIGURE 4.20

Junction-depth measurement by the groove-and-stain technique. The distances a and b are measured through a microscope, and the junction depth is calculated using Eq. (4.11).

Junction Depth Measurement



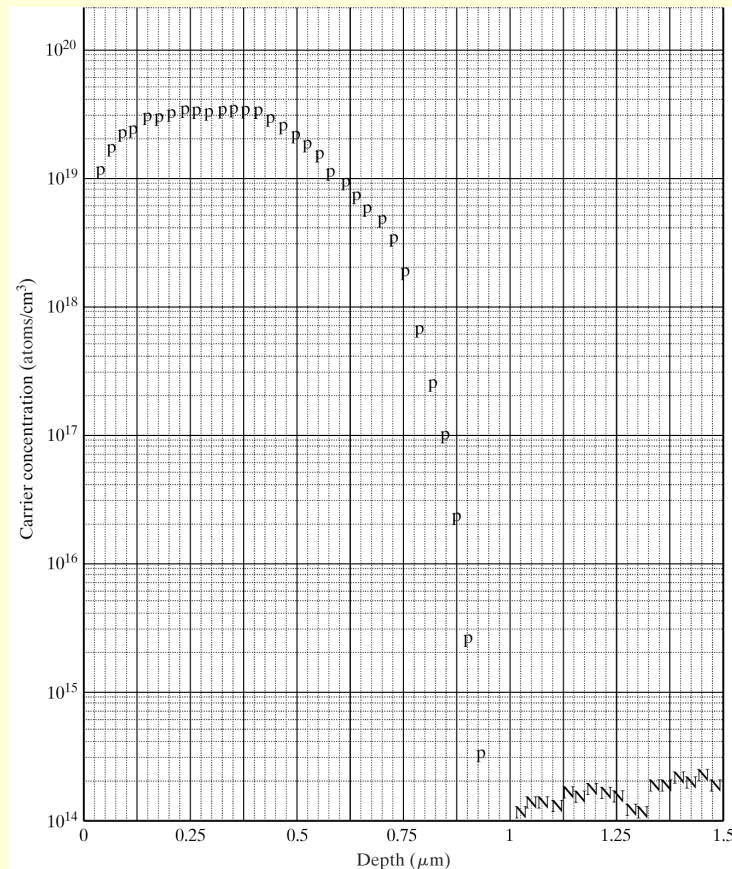
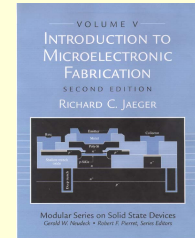
- Angle Lap Technique

$$x_j = d \tan \theta = N \frac{\lambda}{2}$$

FIGURE 4.21

Junction depth measurement by the angle-lap and stain method. Interference fringe lines are used to measure the distance d , which is related to the junction depth using Eq. (4.12).

Impurity Profiling Spreading Resistance



- Region of Interest is Angle-Lapped
- Two-Point Probe Resistance Measurements vs. Depth
- Profile Extracted

FIGURE 4.22

Example of an impurity profile measured using the spreading resistance method.

Impurity Profiling

Secondary Ion Mass Spectroscopy (SIMS)

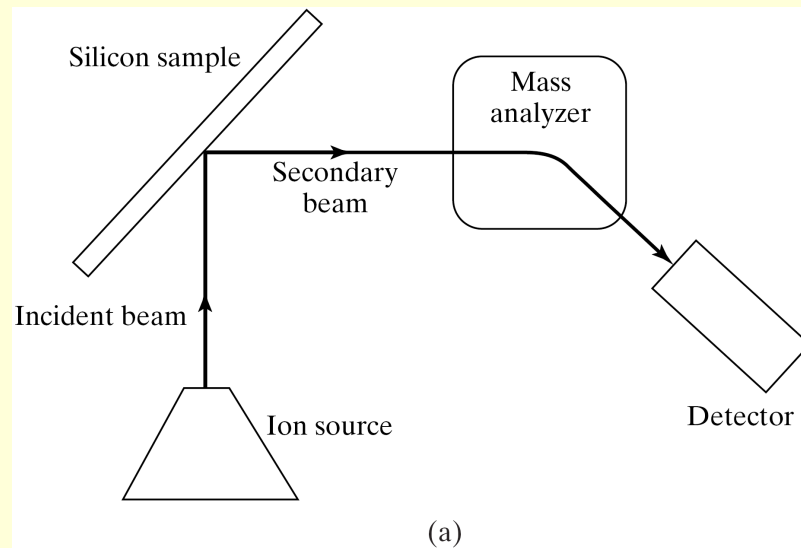
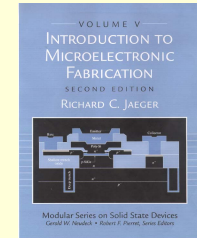


TABLE 4.3 SIMS Analysis in Silicon.

Element	Ion Beam	Sensitivity
Arsenic	Cesium	$5 \times 10^{14}/\text{cm}^3$
Boron	Oxygen	$1 \times 10^{13}/\text{cm}^3$
Phosphorus	Cesium	$5 \times 10^{15}/\text{cm}^3$
Oxygen	Cesium	$1 \times 10^{17}/\text{cm}^3$

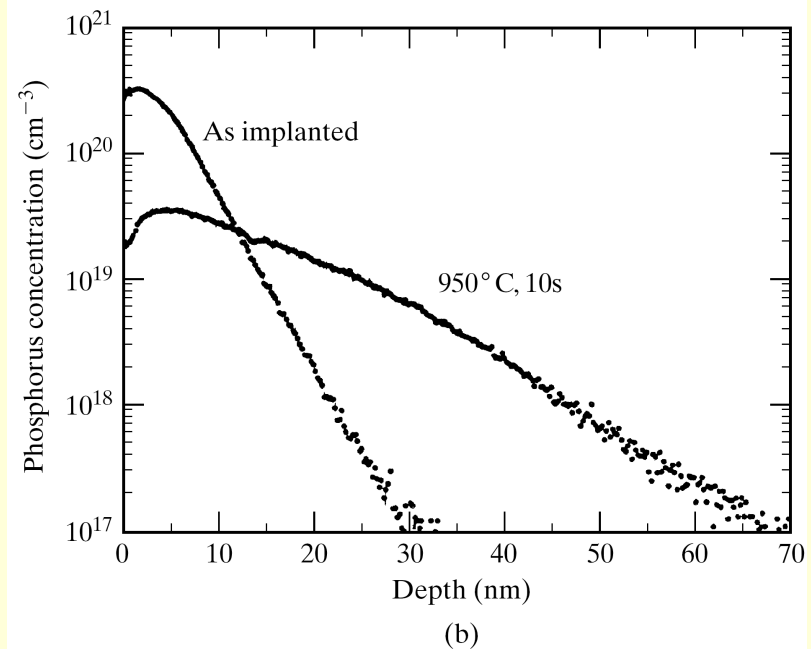


FIGURE 4.23

(a) Concept of a SIMS analysis system. (b) Example of an impurity profile measured using the SIMS analysis. Copyright 1997 IEEE. Reprinted with permission from Ref. [17].

Diffusion Simulation

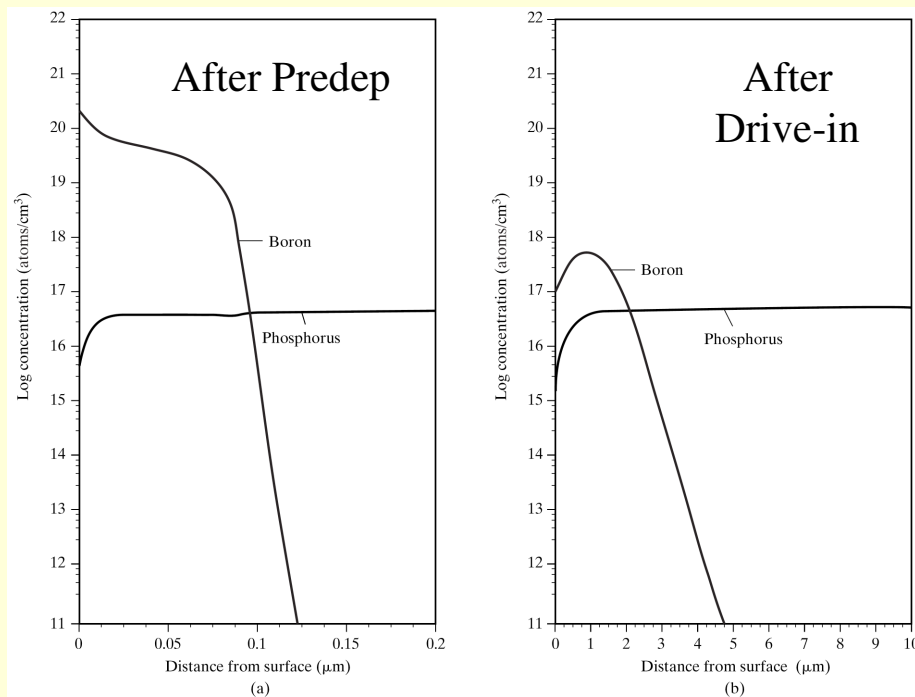
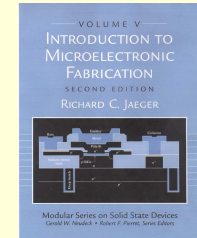
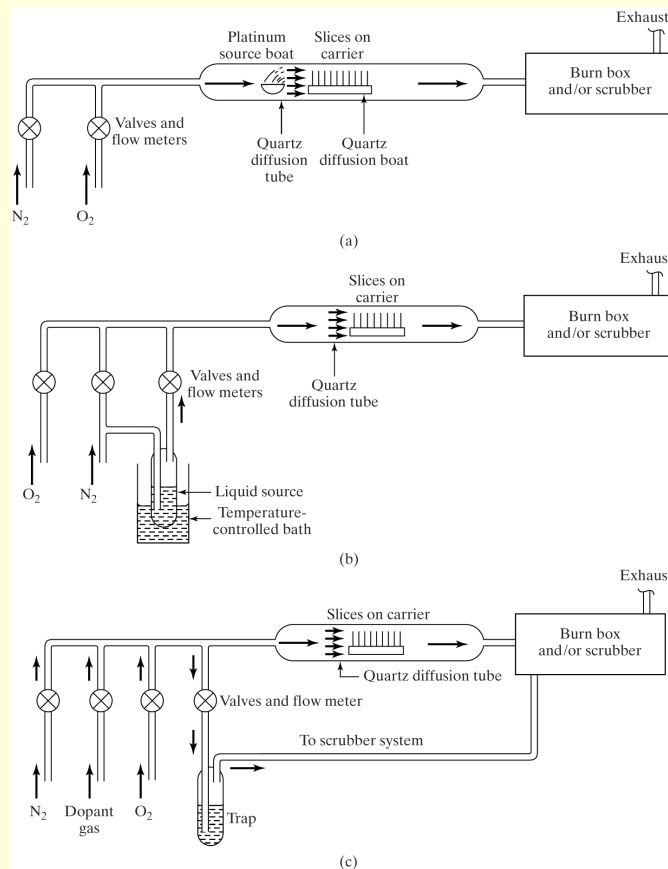
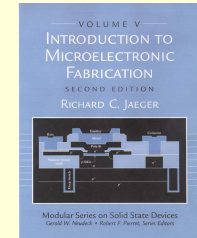


FIGURE 4.24
SUPREM simulation results for two-step boron diffusion into phosphorus doped wafer from Ex. 4.3.

SUPREM Simulation

```
$TWO STEP DIFFUSION
INITIALIZE <100> PHOS=0.18 RESISTIVITY
DIFFUSE TEMP=900 TIME=15 BORON=1E21
...
...
DIFFUSION TEMP=1100 TIME=300
...
...
```

Diffusion Systems



Open Furnace Tube Systems

- (a) Solid source in platinum source boat
- (b) Liquid Source - carrier gas passing through bubbler
- (c) Gaseous impurity source

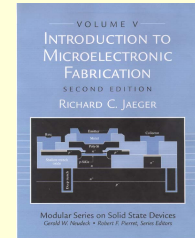
Wafers in Quartz Boat Scrubber at Output

FIGURE 4.25

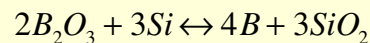
Open-furnace-tube diffusion systems. (a) Solid source in a platinum source boat in the rear of diffusion tube; (b) liquid-source system with carrier gas passing through a bubbler; (c) diffusion system using gaseous impurity sources. Copyright John Wiley and Sons. Reprinted with permission from Ref. [23].

Diffusion Systems

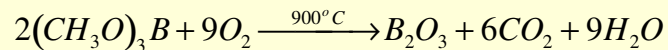
Boron Diffusion



Surface Reaction:

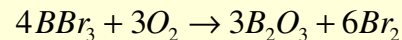


Solid Sources: Boron Nitride & Trimethylborate (TMB)

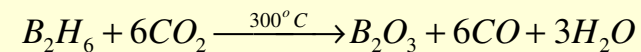
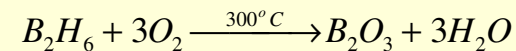


Class is using Boron Nitride Wafers

Liquid Sources: Boron Tribromide BBr_3



Gaseous Source : Diborane B_2H_6 (Extremely Toxic)

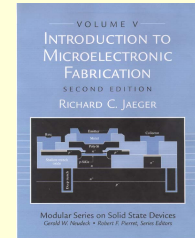


All systems need careful scrubbing!

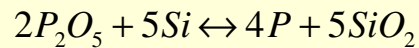


Diffusion Systems

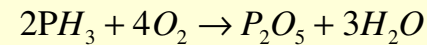
Phosphorus Diffusion



Surface Reaction :



Gaseous Source : Phosphine PH_3 (Extremely Toxic)



Solid Sources :

Phosphorus Pentoxide

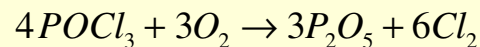
Ammonium monophosphate $NH_4H_2PO_4$

Ammonium diphosphate $(NH_4)_2H_2PO_4$

All systems need careful scrubbing!

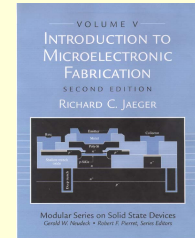


Liquid Source : Phosphorus Oxychloride $POCl_3$

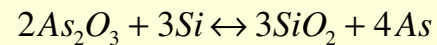


Diffusion Systems

Arsenic & Antimony Diffusion



Arsenic Surface Reaction

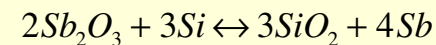


Solid Sources: Possible - Low Surface Concentrations

Gaseous Source: Arsine AsH_3 (Extremely Toxic)

Ion – Implantation Is Normally Used for Deposition

Antimony Surface Reaction



Liquid Source: Antimony Pentachloride Sb_3Cl_5

Ion – Implantation Is Normally Used for Deposition

Diffusion

Toxicity of Gaseous Sources

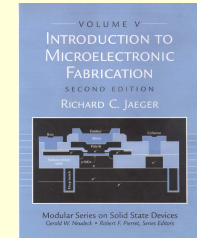


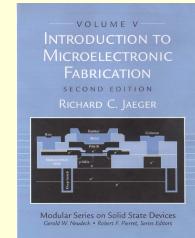
TABLE 4.4 Threshold Limit Recommendations for Common Gaseous Sources [21] *

Source	8-h exposure level (ppm)	Life-threatening exposure	Comments
Diborane (B_2H_6)	0.10	160 ppm for 15 min	Colorless, sickly sweet, extremely toxic, flammable.
Phosphine (PH_3)	0.30	400 ppm for 30 min	Colorless, decaying fish odor, extremely toxic, flammable. A few minutes' exposure to 2000 ppm can be lethal.
Arsine (AsH_3)	0.05	6–15 ppm for 30 min	Colorless, garlic odor, extremely toxic. A few minutes' exposure to 500 ppm can be lethal.
Silane (SiH_4)	0.50	Unknown	Repulsive odor, burns in air, explosive, poorly understood.
Dichlorosilane (SiH_2Cl_2)	5.00	...	Colorless, flammable, toxic. Irritating odor provides adequate warning for voluntary withdrawal from contaminated areas.

Silane and Dichlorosilane Used for Polysilicon Deposition

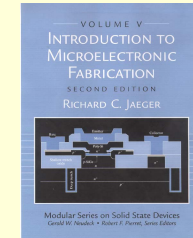
*Data from the 1979 American Conference of Governmental Hygienists (ACGIH).

Diffusion Gettering



- Improves Quality of Wafers
 - Removes Metallic Impurities: Cu, Au, Fe, Ni (Rapid Diffusers)
 - Removes Crystal Defects: Dislocations
- Backside Treatment
 - Surface Damage e. g. Sandblasting
 - Phosphorus Diffusion
- Argon Implantation
- Internal Stress
- Crystal Defects
- Oxygen Incorporation
 - During Growth
 - Implantation

Diffusion References



- [1] R. F. Pierret, *Semiconductor Fundamentals*, Volume I in the Modular Series on Solid State Devices, Addison-Wesley, Reading, MA, 1983.
- [2] R. A. Colclaser, *Microelectronics: Processing and Device Design*, John Wiley & Sons, New York, 1980.
- [3] R. F. Pierret, *Advanced Semiconductor Fundamentals*, Volume VI in the Modular Series on Solid State Devices, Addison-Wesley, Reading, MA, 1987.
- [4] D. P. Kennedy and R. R. O'Brien, "Analysis of the Impurity Atom Distribution Near the Diffusion Mask for a Planar p - n Junction," *IBM Journal of Research and Development*, 9, 179–186 (May, 1965).
- [5] J. C. Irvin, "Resistivity of Bulk Silicon and of Diffused Layers in Silicon," *Bell System Technical Journal*, 41, 387–410 (March, 1962).
- [6] L. R. Weisberg and J. Blanc, "Diffusion with Interstitial-Substitutional Equilibrium: Zinc in GaAs," *Physical Review*, 131, 1548–1552 (August 15, 1963).
- [7] R. B. Fair, "Boron Diffusion in Silicon—Concentration and Orientation Dependence, Background Effects, and Profile Estimation," *Journal of the Electrochemical Society*, 122, 800–805 (June, 1975).
- [8] R. B. Fair, "Profile Estimation of High-Concentration Arsenic Diffusions in Silicon," *Journal of Applied Physics*, 43, 1278–1280 (March, 1972).
- [9] R. B. Fair and J. C. C. Tsai, "Profile Parameters of Implanted-Diffused Arsenic Layers in Silicon," *Journal of the Electrochemical Society*, 123, 583–586 (1976).
- [10] J. C. C. Tsai, "Shallow Phosphorus Diffusion Profiles in Silicon," *Proceedings of the IEEE*, 57, 1499–1506 (September, 1969).
- [11] R. B. Fair and J. C. C. Tsai, "A Quantitative Model for the Diffusion of Phosphorus in Silicon and the Emitter Dip Effect," *Journal of the Electrochemical Society*, 124, 1107–1118 (July, 1977).
- [12] W. R. Runyan, *Semiconductor Measurements and Instrumentation*, McGraw-Hill, New York, 1975.
- [13] L. J. van der Pauw, "A Method of Measuring Specific Resistivity and Hall Effect of Discs of Arbitrary Shape," *Philips Research Reports*, 13, 1–9 (February, 1958).
- [14] R. Chwang, B. J. Smith, and C. R. Crowell, "Contact Size Effects on the van der Pauw Method for Resistivity and Hall Coefficient Measurements," *Solid-State Electronics*, 17, 1217–1227 (December, 1974).
- [15] P. F. Kane, and G. B. Larrabee, *Characterization of Semiconductor Materials*, McGraw-Hill Book Company, New York, 1970.
- [16] (a) C. W. White and W. H. Cristie, "The Use of RBS and SIMS to Measure Dopant Profile Changes in Silicon by Pulsed Laser Annealing," *Solid-State Technology*, pp. 109–116, September 1980. (b) J. M. Anthony et al., "Super SIMS for Ultra Sensitive Impurity Analysis," *Proceedings of the Materials Research Society Symposium* 69, pp. 311–316, 1986.
- [17] A. Agarwal et al., "Boron-enhanced-Diffusion of Boron: The Limiting Factor for Ultra-shallow Junctions," *IEEE IEDM Technical Digest*, pp. 467–470, December 1997.
- [18] D. A. Antoniadis and R. W. Dutton, "Models for Computer Simulation of Complete IC Fabrication Processes," *IEEE Journal of Solid State Circuits*, SC-14, 412–422 (April, 1979).
- [19] C. P. Ho, J. D. Plummer, S. E. Hansen, and R. W. Dutton, "VLSI Process Modeling—SUPREM III," *IEEE Trans. Electron Devices*, ED-30, 1438–1453 (November, 1983).
- [20] D. Chin, M. Kump, H. G. Lee, and R. W. Dutton, "Process Design Using Coupled 2D Process and Device Simulators," *IEEE IEDM Digest*, pp. 223–226 (December, 1980).
- [21] C. D. Maldonado, F. Z. Custode, S. A. Louie, and R. K. Pancholy, "Two Dimensional Simulation of a 2 μ m CMOS Process Using ROMANS II," *IEEE Trans. Electron Devices*, 30, 1462–1469 (November, 1983).
- [22] M. E. Law, C. S. Rafferty, and R. W. Dutton, "New n -well Fabrication Techniques Based on 2D Process Simulation," *IEEE IEDM Digest*, pp. 518–521 (December, 1986).
- [23] R. W. Dutton, "Modeling and Simulation for VLSI," *IEEE IEDM Digest*, pp. 2–7 (December, 1986).
- [24] *Matheson Gas Data Book*, Matheson Gas Products, 1980.
- [25] A. B. Glaser and G. E. Subak-Sharpe, *Integrated Circuit Engineering*, Addison-Wesley, Reading, MA, 1979.
- [26] S. K. Ghandhi, *VLSI Fabrication Principles*, John Wiley & Sons, New York, 1983.
- [27] S. M. Sze, Ed., *VLSI Technology*, McGraw-Hill, New York, 1983.
- [28] S. K. Ghandhi, *The Theory and Practice of Microelectronics*, John Wiley & Sons, New York, 1968.
- [29] R. B. Fair, "Recent Advances in Implantation and Diffusion Modeling for the Design and Process Control of Bipolar ICs," *Semiconductor Silicon 1977*, PV 77-2, pp. 968–985.
- [30] F. M. Smits, "Measurement of Sheet Resistivities with the Four Point Probe," *Bell System Technical Journal*, 37, 711–718 (May, 1958).
- [31] W. R. Runyan and K. E. Bean, *Semiconductor Integrated Circuit Processing Technology*, Addison Wesley Publishing Company, Reading, MA, 1990.

End of Chapter 4

Introduction to Microelectronic Fabrication

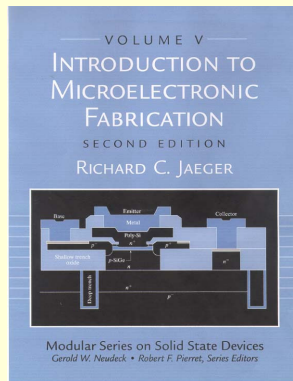
by

Richard C. Jaeger

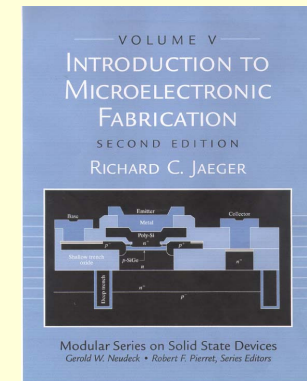
Distinguished University Professor
ECE Department

Auburn University

Chapter 5 Ion Implantation

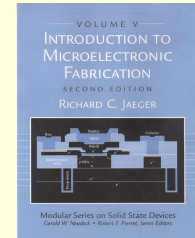


© 2002 Pearson Education, Inc., Upper Saddle River, NJ. All rights reserved.
This material is protected under all copyright laws as they currently exist. No
portion of this material may be reproduced, in any form or by any means,
without permission in writing from the publisher.



For the exclusive use of adopters of the book
Introduction to Microelectronic Fabrication,
Second Edition by Richard C. Jaeger. ISBN0-201-
44494-1.

Copyright Notice



- © 2002 Pearson Education, Inc., Upper Saddle River, NJ. All rights reserved. This material is protected under all copyright laws as they currently exist. No portion of this material may be reproduced, in any form or by any means, without permission in writing from the publisher.
- For the exclusive use of adopters of the book Introduction to Microelectronic Fabrication, Second Edition by Richard C. Jaeger. ISBN0-201-44494-1.

Ion Implantation

High Energy Accelerator

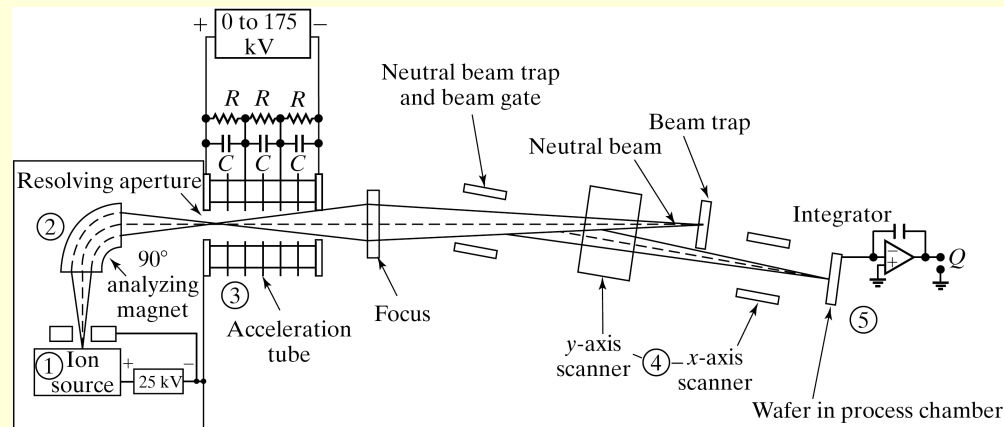
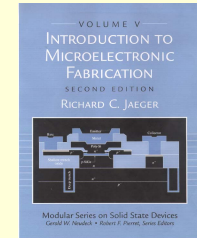


FIGURE 5.1
Schematic drawing of a typical ion implanter

1. Ion Source
2. Mass Spectrometer
3. High-Voltage Accelerator (Up to 5 MeV)
4. Scanning System
5. Target Chamber

Force on charged particle $\vec{F} = q(\vec{v} \times \vec{B})$

Magnetic Field $|\vec{B}| = \sqrt{\frac{2mV}{qr^2}}$

Implanted Dose $Q = \frac{1}{mqA} \int_0^T I(t) dt$

m = mass

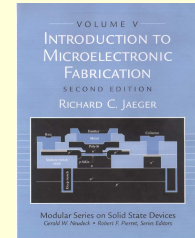
\vec{v} = velocity

V = acceleration potential

A = wafer area

Ion Implantation

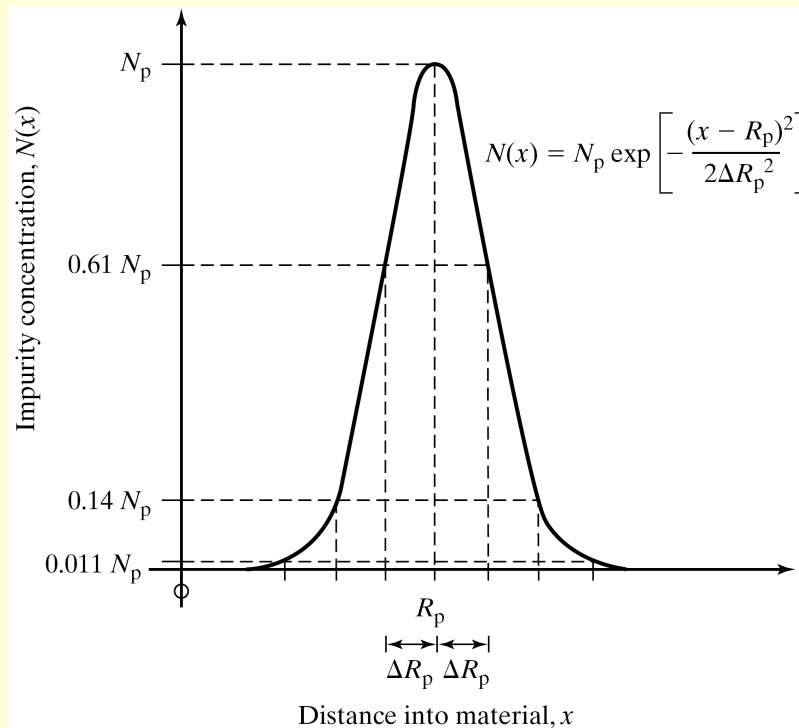
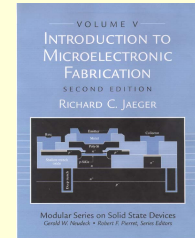
Overview



- Wafer is Target in High Energy Accelerator
- Impurities “Shot” into Wafer
- Preferred Method of Adding Impurities to Wafers
 - Wide Range of Impurity Species (Almost Anything)
 - Tight Dose Control (A few % vs. 20-30% for high temperature pre-deposition processes)
 - Low Temperature Process
- Expensive Systems
- Vacuum System

Ion Implantation

Mathematical Model



Gaussian Profile

$$N(x) = N_p \exp \left[-\frac{(x - R_p)^2}{2\Delta R_p^2} \right]$$

R_p = Projected Range

ΔR_p = Straggle

Dose

$$Q = \int_0^{\infty} N(x) dx = \sqrt{2\pi} N_p \Delta R_p$$

Ion Implantation

Projected Range

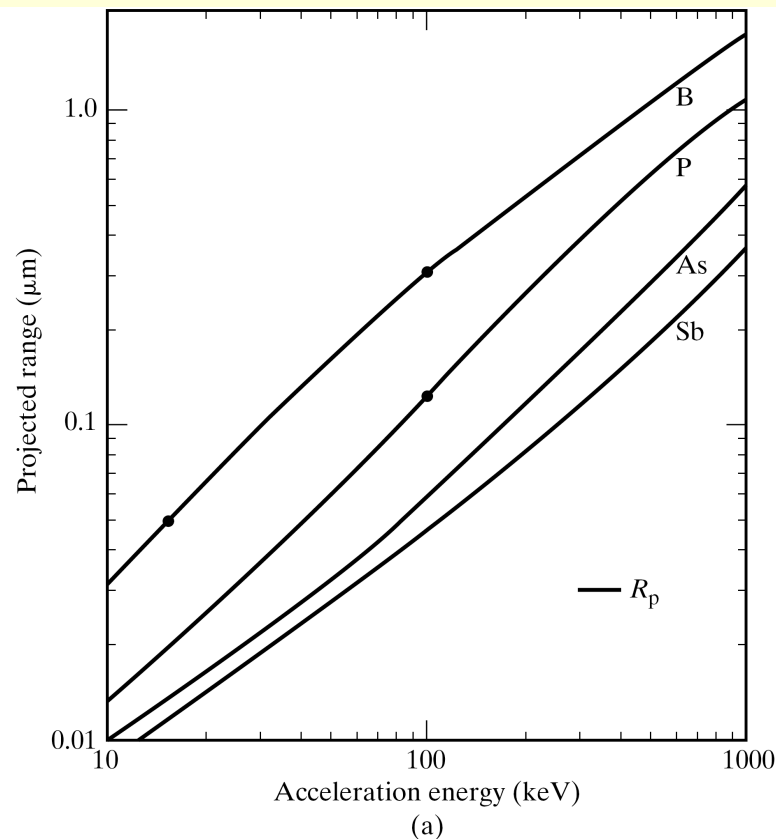
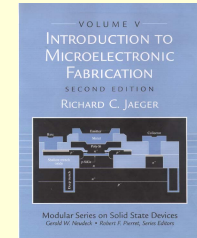


FIGURE 5.3

Projected range and straggle calculations based on LSS theory. (a) Projected range R_p for boron, phosphorus, arsenic, and antimony in amorphous silicon. Results for SiO_2 and for silicon are virtually identical. (b) Vertical σ_p and transverse σ_t straggle for boron, phosphorus, arsenic, and antimony. Reprinted with permission from Ref. [2]. (Copyright van Nostrand Reinhold Company, Inc.)

Ion Implantation Straggle

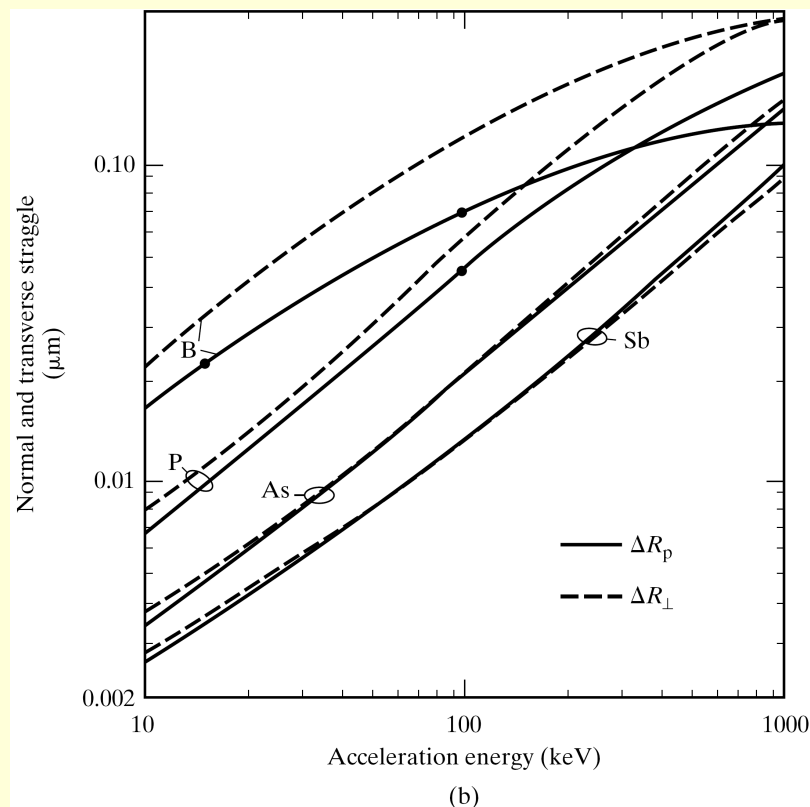
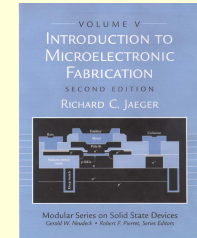
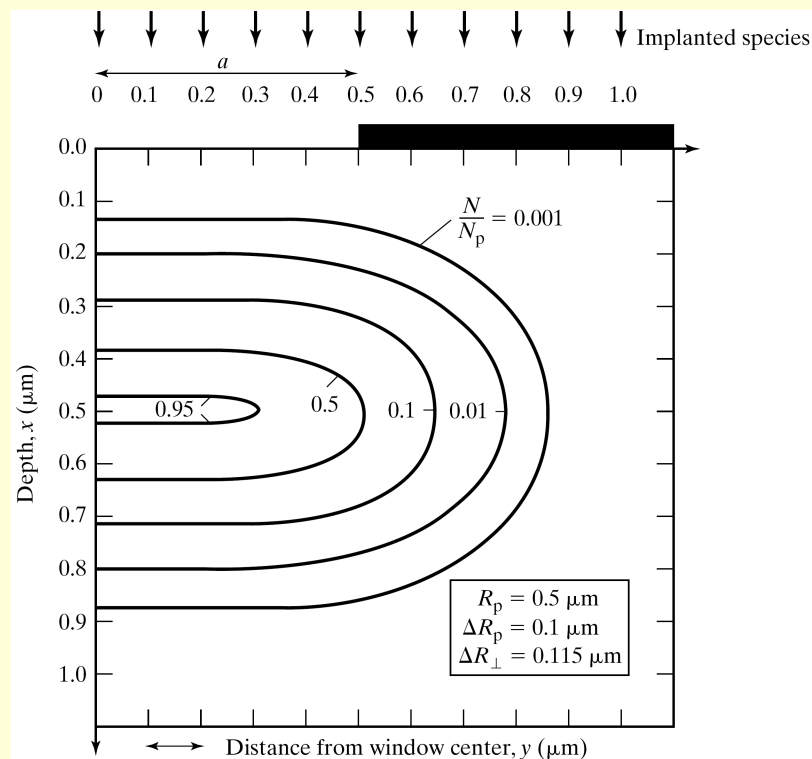
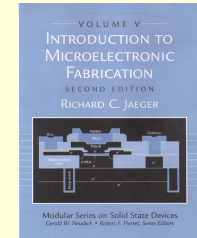


FIGURE 5.3

Projected range and straggle calculations based on LSS theory. (a) Projected range R_p for boron, phosphorus, arsenic, and antimony in amorphous silicon. Results for SiO_2 and for silicon are virtually identical. (b) Vertical R_p and transverse R_l straggle for boron, phosphorus, arsenic, and antimony. Reprinted with permission from Ref. [2]. (Copyright van Nostrand Reinhold Company, Inc.)

Ion Implantation

Selective Implantation



$$N(x, y) = N(x)F(y)$$

$$F(y) = \frac{1}{2} \left[\operatorname{erfc} \left(\frac{y-a}{\sqrt{2}\Delta R_{\perp}} \right) - \operatorname{erfc} \left(\frac{y+a}{\sqrt{2}\Delta R_{\perp}} \right) \right]$$

ΔR_{\perp} = transverse straggle

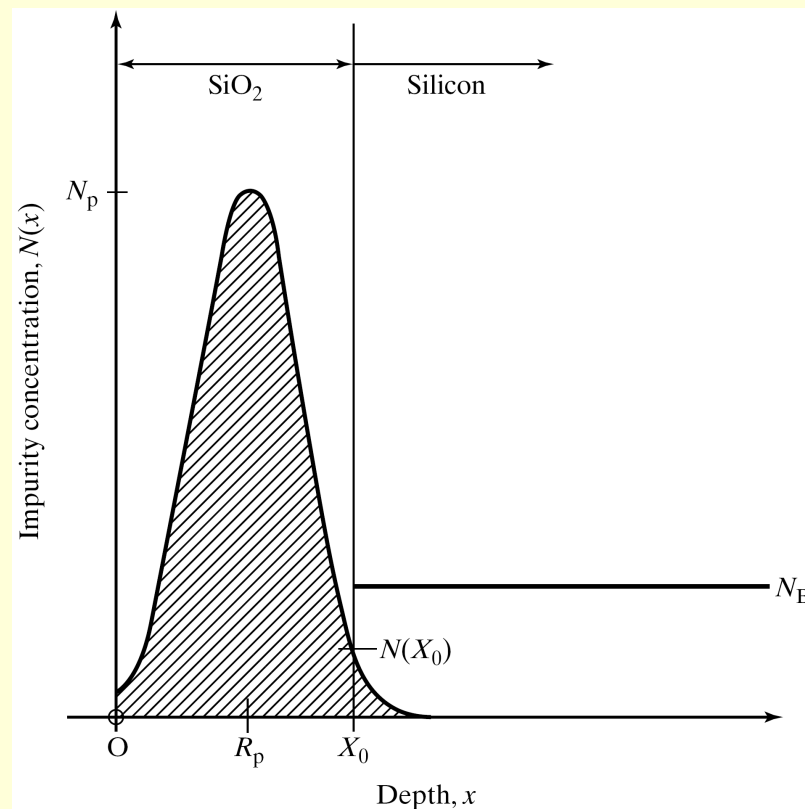
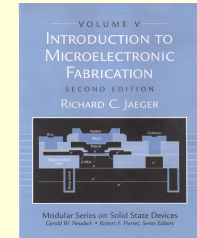
$N(x)$ is one - dimensional solution

Figure 5.4

Contours of equal ion concentration for an implantation into silicon through a 1- μm window. The profiles are symmetrical about the x-axis and were calculated using the equation above taken from Ref. [3].

Ion Implantation

Selective Implantation



- Desire Implanted Impurity Level to be Much Less Than Wafer Doping

$$N(X_0) \ll N_B$$

or

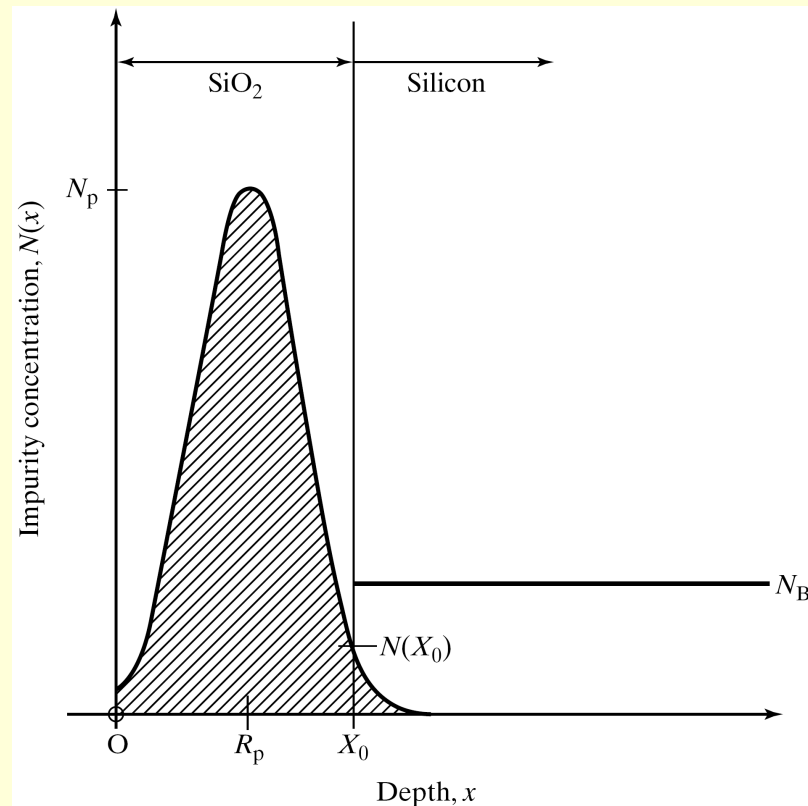
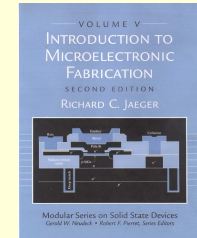
$$N(X_0) < N_B/10$$

FIGURE 5.5

Implanted impurity profile with implant peak in the oxide. The barrier material must be thick enough to ensure that the concentration in the tail of the distribution is much less than N_B .

Ion Implantation

Selective Implantation

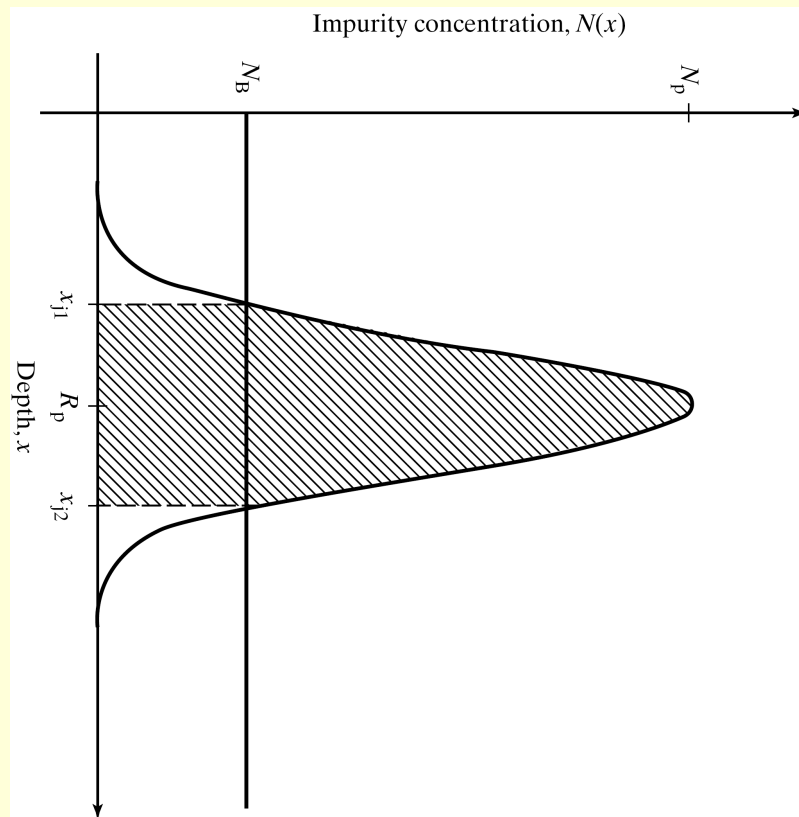
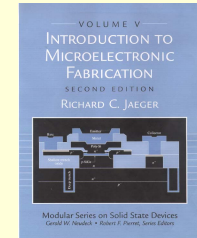


$$X_0 \geq R_p + \Delta R_p \sqrt{2 \ln \left(\frac{10 N_p}{N_B} \right)} = R_p + m \Delta R_p$$

TABLE 5.1 Values of m for Various Values of N_p/N_B .

N_p/N_B	m
10^1	3.0
10^2	3.7
10^3	4.3
10^4	4.8
10^5	5.3
10^6	5.7

Ion Implantation Junction Depth



$$N(x_j) = N_B$$

$$N_p \exp\left[-\frac{(x_j - R_p)^2}{2\Delta R_p^2}\right] = N_B$$

$$x_j = R_p \pm \Delta R_p \sqrt{2 \ln\left(\frac{N_p}{N_B}\right)}$$

FIGURE 5.6

Junction formation by impurity implantation in silicon. Two *pn* junctions are formed at x_{j1} and x_{j2} .

Ion Implantation Channeling

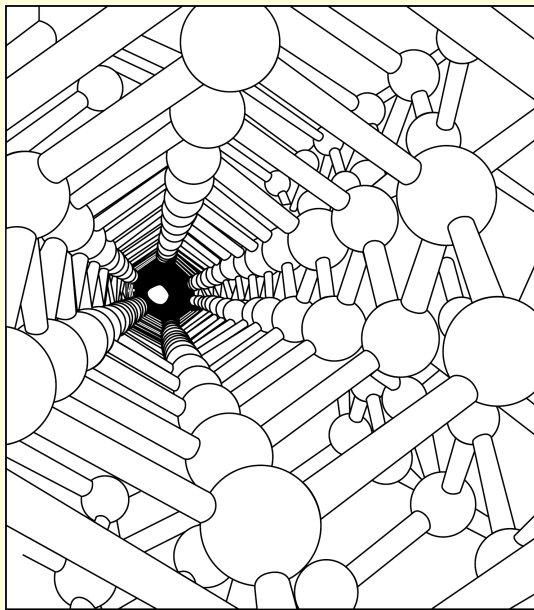
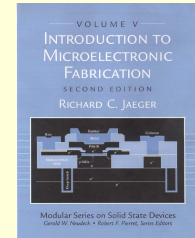


FIGURE 5.7

The silicon lattice viewed along the {110} axis. From *THE ARCHITECTURE OF MOLECULES* by Linus Pauling and Roger Hayward. Copyright © 1964 W. H. Freeman and Company. Reprinted with permission from Refs. [4a] and [4b].

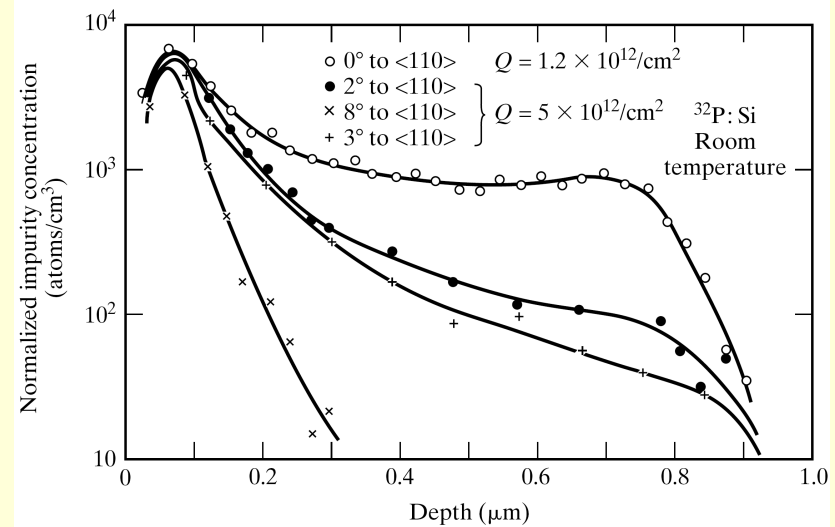
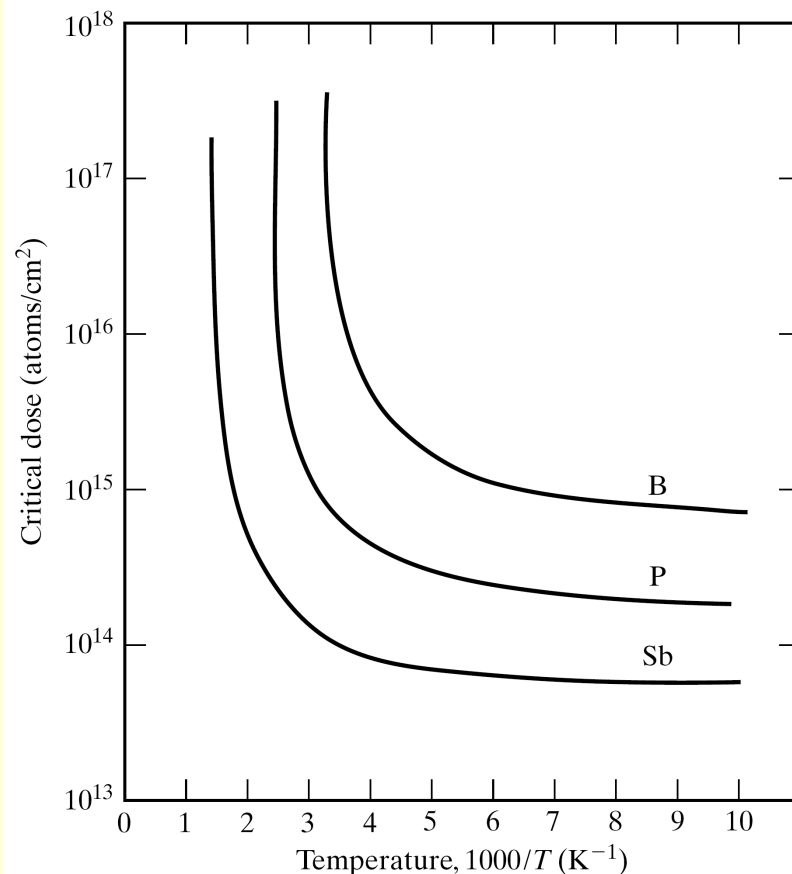
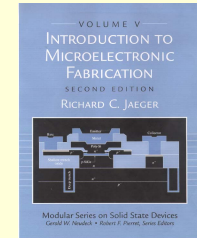


FIGURE 5.8

Phosphorus impurity profiles for 40-keV implantations at various angles from the axis. Copyright 1968 by national Research Council of Canada. Reprinted with permission from Ref. [5].

Ion Implantation

Lattice Damage and Annealing



- Implantation Causes Damage to Surface
- Typically Removed by Annealing Cycle 800-1000° C for 30 min.
- Rapid Thermal Annealing (RTA) Now Used for Lower Dt Product

FIGURE 5.9

A plot of the dose required to form an amorphous layer on silicon versus reciprocal target temperature. Arsenic falls between phosphorus and antimony. Copyright 1970 by Plenum Publishing Corporation. Reprinted with permission from Ref. [6].

Ion Implantation

Deviation from Gaussian Theory

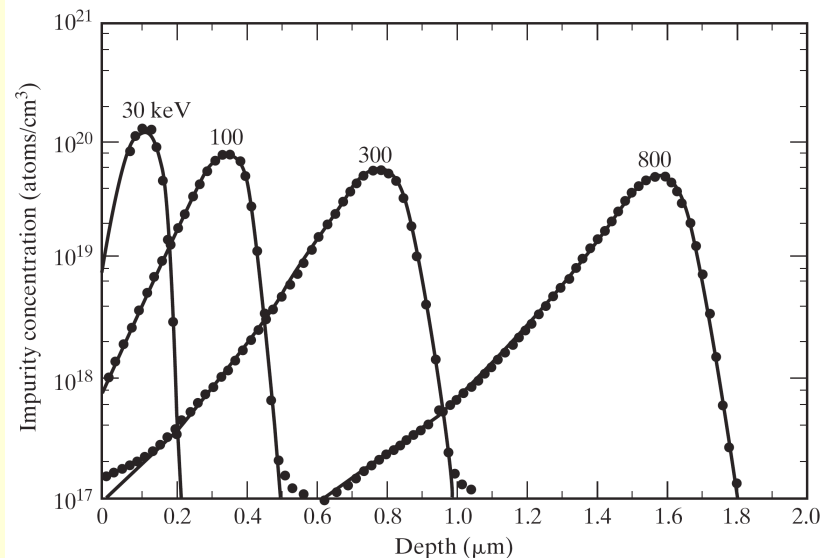
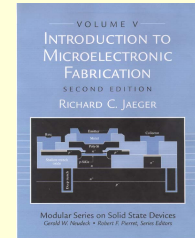


FIGURE 5.10

Measured boron impurity distributions compared with four-moment (Pearson IV) distribution functions. The boron was implanted into amorphous silicon without annealing. Reprinted with permission from Philips Journal of Research [8].

- Curves Deviate from Gaussian for Deeper Implantations (> 200 keV)
- Curves Fit Four-Moment (Pearson Type-IV) Distribution Functions

Ion Implantation

Shallow Implantation

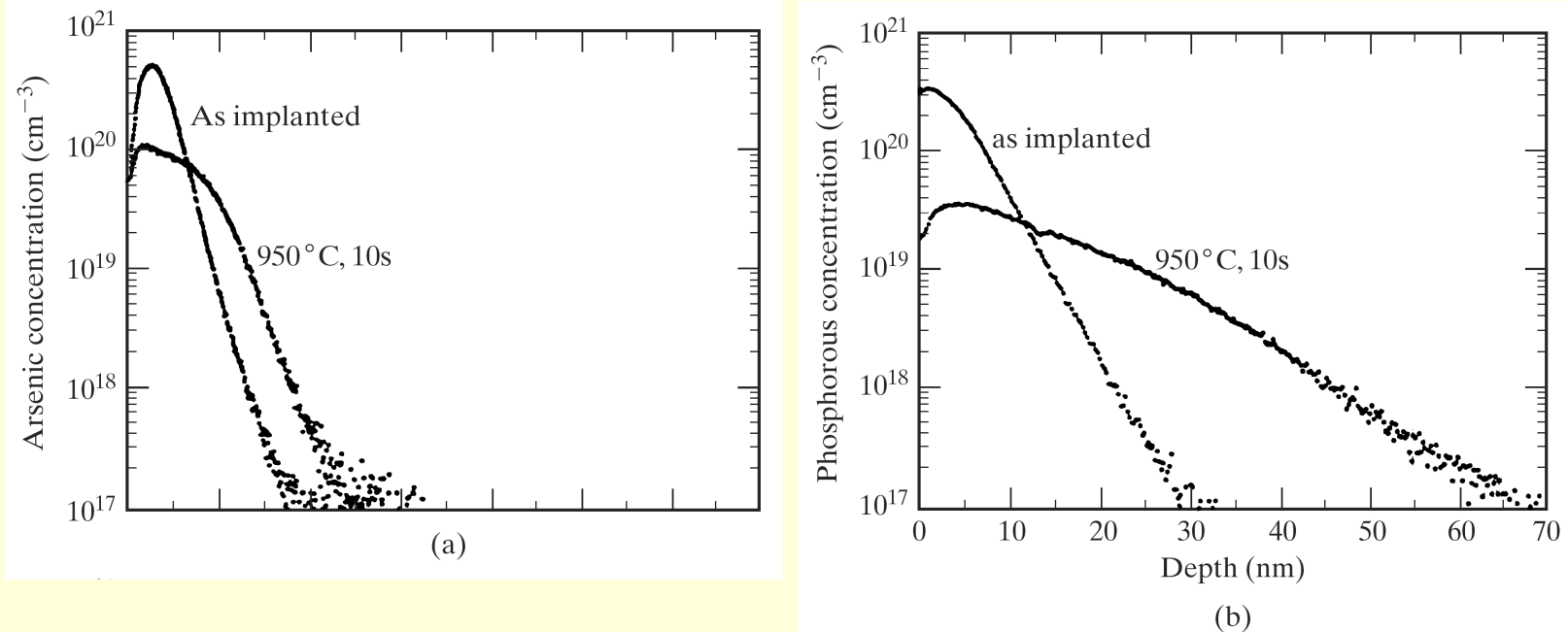
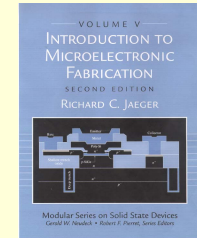


FIGURE 5.11

Examples of transient enhanced diffusion. SIMS data comparing as-implanted and annealed depth profiles from (a) $3 \times 10^{14}/\text{cm}^2$, 2 keV As^+ , and (b) $3 \times 10^{14}/\text{cm}^2$, 1 keV P^+ . Annealing conditions were 950°C for 10 sec. SIMS depth profiles of $1 \times 10^{15}/\text{cm}^2$ B implanted at 0.5-, 1-, 2-, and 5 keV (c) as-implanted, and (d) after annealing at 1050°C for 10 sec. Copyright 1997 IEEE. Reprinted with permission from Ref. [13].

Ion Implantation

Shallow Implantation

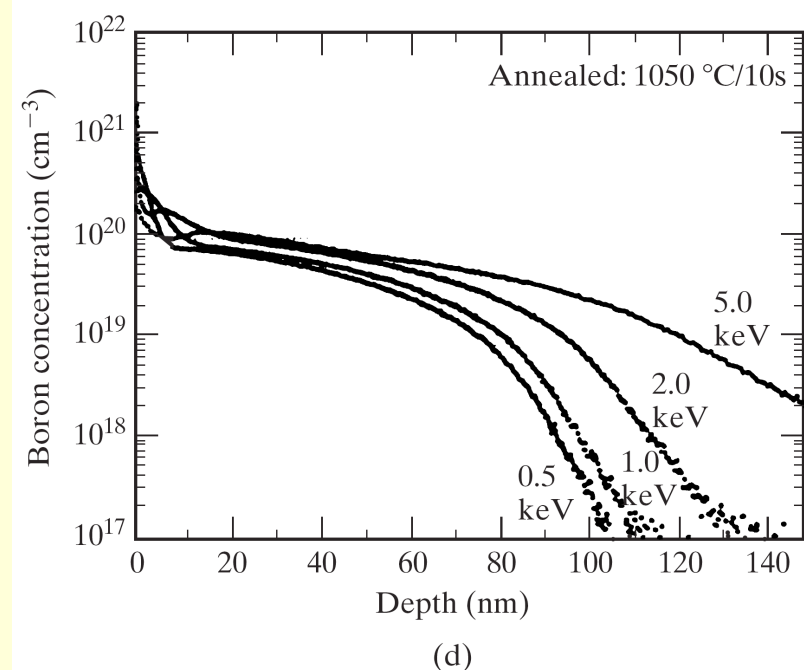
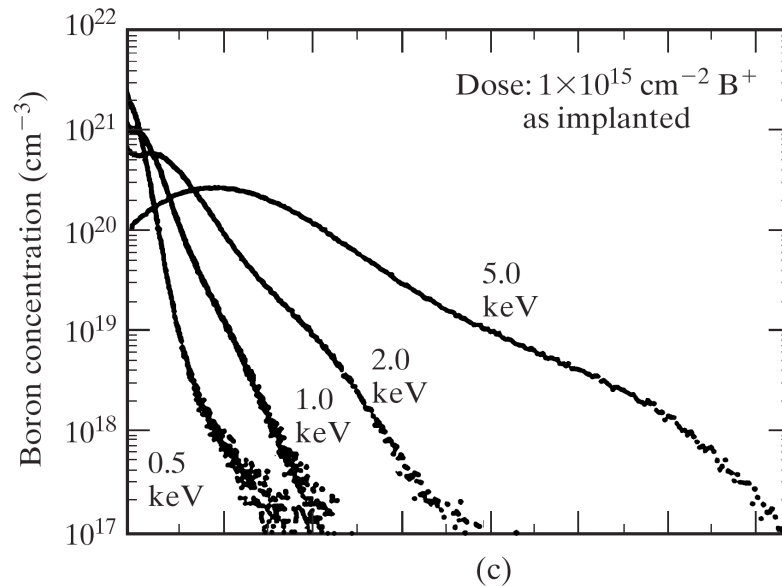
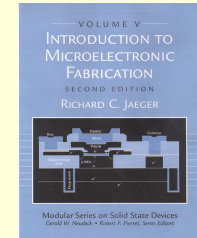
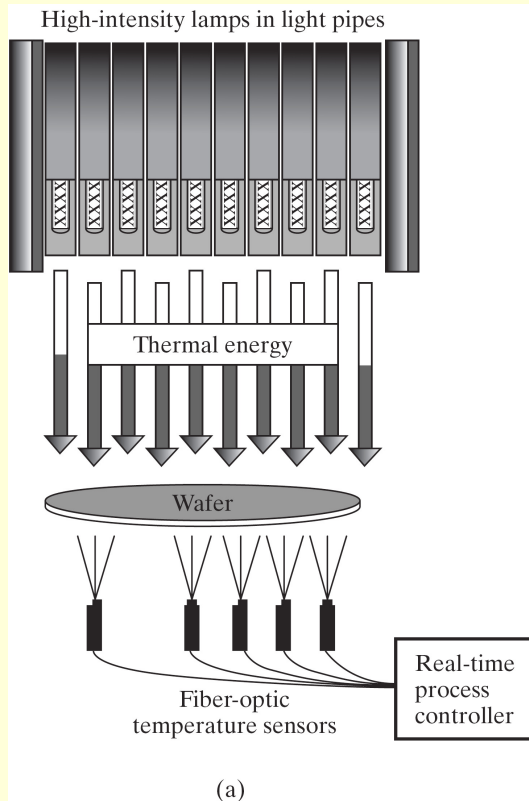
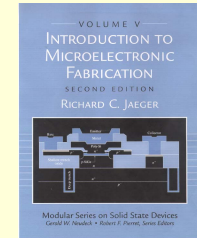


FIGURE 5.11

Examples of transient enhanced diffusion. SIMS data comparing as-implanted and annealed depth profiles from (a) $3 \times 10^{14}/\text{cm}^2$, 2 keV As^+ , and (b) $3 \times 10^{14}/\text{cm}^2$, 1 keV P^+ . Annealing conditions were 950°C for 10 sec. SIMS depth profiles of $1 \times 10^{15}/\text{cm}^2$ B implanted at 0.5-, 1-, 2-, and 5 keV (c) as-implanted, and (d) after annealing at 1050°C for 10 sec. Copyright 1997 IEEE. Reprinted with permission from Ref. [13].

Ion Implantation

Rapid Thermal Annealing



- Rapid Heating
- 950-1050° C
- 50° C/sec
- Very Low Dt

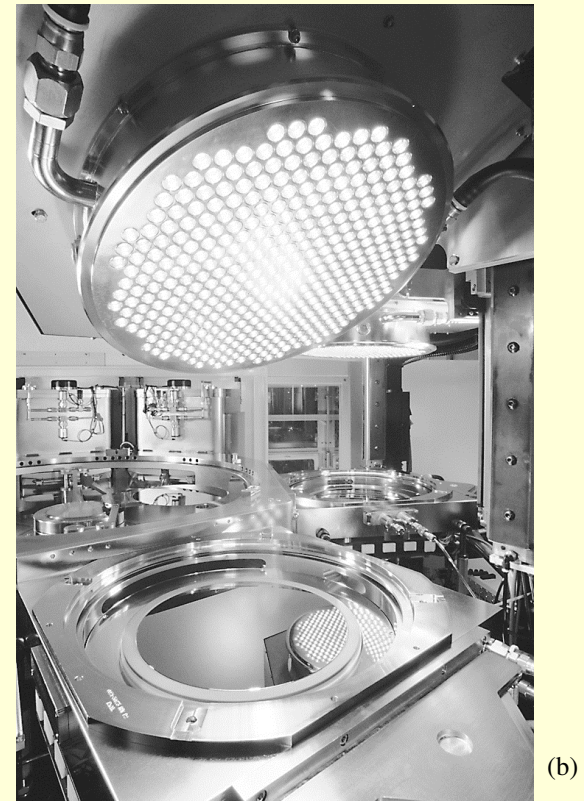
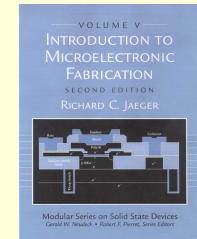


Figure 5.12

(a) Concept for a rapid thermal annealing (RTP) system. (b) Applied Materials 300 mm RTP System (Courtesy Applied Materials)

Ion Implantation

References



- [1] J. Lindhard, M. Scharff, and H. Schiott, "Range Concepts in Heavy Ion Ranges," *Mat.-Fys. Med. Dan. Vid. Selsk.*, 33, No. 14, 1963.
- [2] J. F. Gibbons, W. S. Johnson, and S. W. Mylroie, *Projected Range in Semiconductors*, Second Edition, Dowden, Hutchinson, and Ross, New York, 1975.
- [3] (a) L. Pauling and R. Hayward, *The Architecture of Molecules*, W. H. Freeman, San Francisco, 1964. (b) S. M. Sze, Ed., *Semiconductor Devices Physics and Technology*, McGraw-Hill, New York, 1985.
- [4] S. Furukawa, H. Matsumura, and H. Ishiura, "Lateral Distribution Theory of Implanted Ions," in S. Namba, Ed., *Ion Implantation in Semiconductors*, Japanese Society for the Promotion of Science, Kyoto, p. 73 (1972).
- [5] G. Dearnaley, J. H. Freeman, G. A. Card, and M. A. Wilkins, "Implantation Profiles of ^{32}P Channeled into Silicon Crystals," *Canadian Journal of Physics*, 46, 587–595 (March 15, 1968).
- [6] F. F. Morehead and B. L. Crowder, "A Model for the Formation of Amorphous Si by Ion Implantation," p. 25–30, in Eisen and Chadderton (see Source Listing 4).
- [7] B. L. Crowder and F. F. Morehead, Jr., "Annealing Characteristics of n -type Dopants in Ion-Implanted Silicon," *Applied Physics Letters*, 14, 313–315 (May 15, 1969).
- [8] W. K. Hofker, "Implantation of Boron in Silicon," *Philips Research Reports Supplements*, No. 8, 1975.
- [9] J. F. Gibbons, "Ion-Implantation in Semiconductors—Part I: Range Distribution Theory and Experiment," *Proceedings of the IEEE*, 56, 295–319 (March, 1968).
- [10] J. F. Gibbons, "Ion Implantation in Semiconductors—Part II: Damage Production and Annealing," *Proceedings of the IEEE*, 60, 1062–1096 (September, 1972).
- [11] T. Hirao, G. Fuse, K. Inoue, S. Takayanagi, Y. Yaegashi, S. Ichikawa, and T. Izumi, "Electrical Properties of Si Implanted with As Through SiO_2 Films," *Journal of Applied Physics*, 51, 262–268 (January, 1980).
- [12] K. Goto, J. Matsuo, Y. Tada, T. Tanaka, Y. Momiyama, T. Sugii, I. Yamada, "A High Performance 50 nm PMOSFET Using Decaborane ($\text{B}_{10}\text{H}_{14}$) Ion Implantation and 2-step Activation Annealing Process," *IEEE IEDM Digest*, pp. 471–474, December 1997.
- [13] A. Agarwal, D. J. Eaglesham, H.-J. Gossman, L. Pelaz, S. B. Herner, D. C. Jacobson, T. E. Haynes, Y. Erokhin, and R. Simonton, "Boron-Enhanced-Diffusion of Boron: The Limiting Factor for Ultra Shallow Junctions," *IEEE IEDM Digest*, pp. 467–470, December 1997.
- [14] A. D. Lilak, S. K. Earles, K. S. Jones, M. E. Law and M. D. Giles, "A Physics-based Modeling Approach for the Simulation of Anomalous Boron Diffusion and Clustering Behavior," *IEEE IEDM Digest*, pp. 493–496, December 1997.
- [15] K. Suzuki, T. Miyashita and Y. Tada, "Damage Calibration Concept and Novel B Cluster Reaction Model for B Transient Enhanced Diffusion Over Thermal Process Range from 600 °C (839 h) to 1,100 °C (5 s) with Various Ion Implantation Doses and Energies," *IEEE IEDM Digest*, pp. 501–504, December 1997.
- [16] S. S. Yu, H. W. Kennel, M. D. Giles and P. A. Packan, "Simulation of Transient Enhanced Diffusion Using Computationally Efficient Models," *IEEE IEDM Digest*, pp. 509–512, December 1997.

SOURCE LISTING

- [1] J. W. Mayer, L. Eriksson, and J. A. Davies, *Ion-Implantation in Semiconductors*, Academic Press, New York, 1970.
- [2] G. Dearnaley, J. H. Freeman, R. S. Nelson, and J. Stephen, *Ion-Implantation*, North-Holland, New York, 1973.
- [3] G. Carter and W. A. Grant, *Ion-Implantation of Semiconductors*, John Wiley & Sons, New York, 1976.
- [4] F. Eisen and L. Chadderton, Eds., *Ion Implantation in Semiconductors*, First International Conference (Thousand Oaks, CA), Gordon and Breach, New York, 1970.
- [5] I. Ruge and J. Graul, Eds., *Ion Implantation in Semiconductors*, Second International Conference (Garmisch-Partenkirchen, West Germany), Springer-Verlag, Berlin, 1972.
- [6] B. L. Crowder, Ed., *Ion Implantation in Semiconductors*, Third International Conference (Yorktown Heights, NY), Plenum, New York, 1973.
- [7] S. Namba, Ed., *Ion Implantation in Semiconductors*, Fourth International Conference (Osaka, Japan), Plenum, New York, 1975.
- [8] F. Chernow, J. Borders, and D. Bruce, Eds., *Ion Implantation in Semiconductors*, Fifth International Conference (Boulder, CO), Plenum, New York, 1976.

End of Chapter 5